自治医科大学　　永井正　業績リスト

発表者名	論文タイトル名	発表誌名	巻号	ページ	出版年
Meguro A, Ozaki K, Sato K, Oh I, Fujiwara S, Hosonuma R, Sasazaki M, Kikuchi Y, Hirata Y, Yamamoto C, Uesawa M, Kobayashi H, Matsu H, Okabe H, Uehara E, Nishikawa A, Tatara R, Hatano K, Yamamoto C, Matsuyama T, Toshima M, Ueda M, Ohmine K, Suzuki T, Mori M, Nagai T, Muroi K & Ozawa K	Rituximab plus 70% cyclophosphamide, doxorubicin, vincristine and prednisone for Japanese patients with diffuse large B-cell lymphoma aged 70 years and older	Leuk Lymphoma	53	43-49	2012
Ohnishi K, Nakaseko C, Takeuchi J, Fujisawa S, Nagai T, Yamazaki H, Tauchi T, Imai K, Mori N, Yagasaki F, Maeda Y, Usui N, Miyamura K, Kiyoi H, Ohtake S & Naoe T	Long-term outcome following imatinib therapy for chronic myelogenous leukemia, with assessment of dosage and blood levels	Cancer Sci	103	1071-1078	2012
Oka S, Muroi K, Yokote T, Fujiwara S, Oh I, Matsuyama T, Ohmine K, Suzuki T, Ozaki K, Mori M, Nagai T, Ozawa K & Hanafusa T	Prediction of progression from refractory anemia by analysis of bone marrow blast cell composition	J Clin Exp Hematop		in press	
Oka S, Muroi K, Fujiwara S, Oh I, Matsuyama T, Ohmine K, Suzuki T, Ozaki K, Mori M, Nagai T, Ozawa K & Hanafusa T	Prediction of progression from refractory cytopenia with unilineage dysplasia by analysis of bone marrow blast cell composition	J Clin Exp Hematop	52	63-66	2012
Oka S, Muroi K, Sato K, Fujiwara S, Oh I, Matsuyama T, Ohmine K, Suzuki T, Ozaki K, Mori M, Nagai T, Hanafusa T, Fukushima N, Tanaka A & Ozawa K	Flow cytometric analysis of kappa and lambda light chain expression in endoscopic biopsy specimens before the diagnosis of B-cell lymphoma	J Clin Exp Hematop	52	127-131	2012
Sato K, Nagai T, Izumi T, Ohmine K, Ozaki K, Muroi K & Ozawa K	Rituximab-induced interstitial pneumonia due to CD8-positive T-cell infiltration	Acta Haematol	128	107-109	2012
Kobayashi H, Matsuyama T, Oka S, Fujiwara S, Oh I, Suzuki T, Ozaki K, Mori M, Nagai T, Ozawa K & Muroi K	Autologous hematopoietic recovery with aberrant antigen expression after allogeneic bone marrow transplantation	J Clin Exp Hematop	52	81-83	2012
Usuki K, Tojo A, Maeda Y, Kobayashi Y, Matsuda A, Ohyashiki K, Nakaseko C, Tatsuya K, Tanaka H, Miyamura K, Miyazaki Y, Okamoto S, Oritani K, Okada M, Usio N, Nagai T, Amagasaki T, Wanajo A & Naoe T	Efficacy and safety of nilotinib in Japanese patients with imatinib-resistant or –intolerant Ph+CML or relapsed/refractory Ph+ALL: a 36-month analysis of a phase I and II study	Int J Hematol	95	409-419	2012

Kobayashi H, Nagai T, Uesawa M, Fujiwara S, Matsuyama T, Sato K, Omine K, Ozaki K, Suzuki T, Mori M, Muroi K, Baley G, Yamamoto H & Ozawa K	Clinical outcome of non-surgical treatment for primary small intestinal lymphoma diagnosed with double-balloon endoscopy	Leuk Lymphoma		Sep 28. [Epub ahead of print]	2012
Fujiwara S, Muroi K, Hirata Y, Sato K, Matsuyama T, Ohmine K, Suzuki T, Ozaki K, Mori M, Nagai T, Tanaka A & Ozawa K	Clinical features of de novo CD25(+) diffuse large B-cell lymphoma. Hematology	Hematology		Sep 12. [Epub ahead of print]	2012
Nagai T, Suzuki T, Komatsu N, Hosokawa K, Nakao S & Ozawa K	Alteration of chromosome 13 abnormalities after therapeutic heamatopoiesis recovery in myelodysplastic syndrome	Open J Hematol		3-7	2012

Transforming mutations of RAC guanosine triphosphatases in human cancers

Masahito Kawazu[a], Toshihide Ueno[b], Kenji Kontani[c], Yoshitaka Ogita[c], Mizuo Ando[a], Kazutaka Fukumura[a], Azusa Yamato[b], Manabu Soda[b], Kengo Takeuchi[d], Yoshio Miki[e], Hiroyuki Yamaguchi[a], Takahiko Yasuda[a,f], Tomoki Naoe[f], Yoshihiro Yamashita[b], Toshiaki Katada[c], Young Lim Choi[a], and Hiroyuki Mano[a,b,g,1]

[a]Department of Medical Genomics, Graduate School of Medicine, University of Tokyo, Tokyo 113-0033, Japan; [b]Division of Functional Genomics, Jichi Medical University, Tochigi 329-0498, Japan; [c]Department of Physiological Chemistry, Graduate School of Pharmaceutical Sciences, University of Tokyo, Tokyo 113-0033, Japan; [d]Pathology Project for Molecular Targets, The Cancer Institute, Japanese Foundation for Cancer Research, Tokyo 135-8550, Japan; [e]Department of Genetic Diagnosis, The Cancer Institute, Japanese Foundation for Cancer Research, Tokyo 135-8550, Japan; [f]Department of Hematology and Oncology, Nagoya University Graduate School of Medicine, Nagoya 466-8550, Japan; and [g]Core Research for Evolutional Science and Technology, Japan Science and Technology Agency, Saitama 332-0012, Japan

Edited by Shuh Narumiya, Kyoto University Faculty of Medicine, Kyoto, Japan, and accepted by the Editorial Board January 9, 2013 (received for review September 22, 2012)

Members of the RAS superfamily of small guanosine triphosphatases (GTPases) transition between GDP-bound, inactive and GTP-bound, active states and thereby function as binary switches in the regulation of various cellular activities. Whereas HRAS, NRAS, and KRAS frequently acquire transforming missense mutations in human cancer, little is known of the oncogenic roles of other small GTPases, including Ras-related C3 botulinum toxin substrate (RAC) proteins. We show that the human sarcoma cell line HT1080 harbors both NRAS(Q61K) and RAC1(N92I) mutant proteins. Whereas both of these mutants were able to transform fibroblasts, knockdown experiments indicated that RAC1(N92I) may be the essential growth driver for this cell line. Screening for RAC1, RAC2, or RAC3 mutations in cell lines and public databases identified several missense mutations for RAC1 and RAC2, with some of the mutant proteins, including RAC1(P29S), RAC1(C157Y), RAC2(P29L), and RAC2(P29Q), being found to be activated and transforming. P29S, N92I, and C157Y mutants of RAC1 were shown to exist preferentially in the GTP-bound state as a result of a rapid transition from the GDP-bound state, rather than as a result of a reduced intrinsic GTPase activity. Activating mutations of RAC GTPases were thus found in a wide variety of human cancers at a low frequency; however, given their marked transforming ability, the mutant proteins are potential targets for the development of new therapeutic agents.

oncogene | resequencing

The identification of transforming proteins and the development of agents that target them have markedly influenced the treatment and improved the prognosis of individuals with cancer. Chronic myeloid leukemia (CML), for example, has been shown to result from the growth-promoting activity of the fusion tyrosine kinase breakpoint cluster region-Abelson murine leukemia viral oncogene homolog 1 (BCR-ABL1), and treatment with a specific ABL1 inhibitor, imatinib mesylate, has increased the 5-y survival rate of individuals with CML to almost 90% (1). Similarly, the fusion of echinoderm microtubule associated protein like 4 gene (*EML4*) to anaplastic lymphoma receptor tyrosine kinase (*ALK*) is responsible for a subset of non–small-cell lung cancer cases (2), and therapy targeted to EML4-ALK kinase activity has greatly improved the progression-free survival of affected individuals compared with that achieved with conventional chemotherapies (3). Therapies that target essential growth drivers in human cancers are thus among the most effective treatments for these intractable disorders.

V-Ki-ras2 Kirsten rat sarcoma viral oncogene homolog (KRAS), v-Ha-ras Harvey rat sarcoma viral oncogene homolog (HRAS), and neuroblastoma RAS viral (v-ras) oncogene homolog (NRAS) are the founding members of the rat sarcoma (RAS) superfamily of small guanosine triphosphatases (GTPases) that is known to comprise >150 members in humans (4). Five subgroups of these small GTPases have been identified and designated as the RAS; ras homolog family member (RHO); RAB1A, member RAS oncogene family (RAB); RAN, member RAS oncogene family (RAN); and ADP-ribosylation factor (ARF) families. All small GTPases function as binary switches that transition between GDP-bound, inactive and GTP-bound, active forms and thereby contribute to intracellular signaling that underlies a wide array of cellular activities, including cell proliferation, differentiation, survival, motility, and transformation (5). Somatic point mutations that activate KRAS, HRAS, or NRAS have been identified in a variety of human tumors, with KRAS being the most frequently activated oncoprotein in humans. Somatic activating mutations of KRAS are thus present in >90% of pancreatic adenocarcinomas, for example (6). Surprisingly, however, mutational activation of small GTPases other than KRAS, HRAS, and NRAS has not been widely reported.

Ras-related C3 botulinum toxin substrate (RAC) 1, RAC2, and RAC3 belong to the RHO family of small GTPases (7). RAC proteins orchestrate actin polymerization, and their activation induces the formation of membrane ruffles and lamellipodia (8), which play essential roles in the maintenance of cell morphology and in cell migration. Accumulating evidence also indicates that RAC proteins function as key hubs of intracellular signaling that underlies cell transformation. RAC1, for example, serves as an essential downstream component of the signaling pathway by which oncogenic RAS induces cell transformation, and artificial introduction of an amino acid substitution (G12V) into RAC1 renders it oncogenic (9). Furthermore, suppression of RAC1 activity induces apoptosis in glioma cells (10), and loss of *RAC1* or *RAC2* results in a marked delay in the development of BCR-ABL1–driven myeloproliferative disorder (11). Despite such important roles of RAC proteins in cancer, somatic transforming mutations of these proteins have not been identified in cancer specimens.

We have now discovered a mutant form of RAC1 with the amino acid substitution N92I in a human sarcoma cell line, HT1080, and have found that this mutation renders RAC1 constitutively active and highly oncogenic. Even though HT1080 cells also harbor the NRAS(Q61K) oncoprotein, RAC1(N92I) is the essential growth driver in this cell line, given that RNA interference (RNAi)-

Author contributions: M.K. and H.M. designed research; M.K., T.U., K.K., Y.O., M.A., K.F., A.Y., M.S., K.T., Y.M., H.Y., T.Y., T.N., Y.Y., T.K., and Y.L.C. performed research; M.K., T.U., K.K., Y.O., K.T., T.N., T.K., Y.L.C., and H.M. analyzed data; and H.M. wrote the paper.

The authors declare no conflict of interest.

This article is a PNAS Direct Submission. S.N. is a guest editor invited by the Editorial Board.

[1]To whom correspondence should be addressed. E-mail: hmano@m.u-tokyo.ac.jp.

This article contains supporting information online at www.pnas.org/lookup/suppl/doi:10.1073/pnas.1216141110/-/DCSupplemental.

mediated knockdown of RAC1(N92I) markedly suppressed cell growth. Further screening for *RAC1*, *RAC2*, and *RAC3* mutations among cancer cell lines as well as public databases identified additional transforming mutations of RAC1 and RAC2. Our data thus reveal oncogenic amino acid substitutions for the RAC subfamily of small GTPases in human cancer.

Results

Discovery of the RAC1(N92I) Oncoprotein. To identify transforming genes in the fibrosarcoma cell line HT1080 (12), we isolated cDNAs for cancer-related genes (n = 906) from HT1080 cells and subjected them to deep sequencing with the Genome Analyzer IIx (GAIIx) system. Quality filtering of the 92,025,739 reads obtained yielded 45,325,377 unique reads that mapped to 843 (93.0%) of the 906 target genes. The mean read coverage for the 843 genes was 495× per nucleotide, and ≥70% of the captured regions for 568 genes were read at ≥10× coverage.

Screening for nonsynonymous mutations in the data set with the use of our computational pipeline (13) revealed a total of five missense mutations with a threshold of ≥30× coverage and a ≥30% mutation ratio (Table S1). One of these mutations, a heterozygous missense mutation of *NRAS* that results in a Gln-to-Lys substitution at amino acid position 61 (Q61K), was described previously in this cell line (14) and is the most frequent transforming mutation of *NRAS* (5). We also discovered a missense mutation in another small GTPase, RAC1 (Fig. S1 and Table S1). An A-to-T transversion at position 516 of human *RAC1* cDNA (GenBank accession no. NM_006908.4), resulting in an Asn-to-Ile substitution at position 92 of the encoded protein, was thus identified in 11,525 (47.5%) of the 24,238 total reads covering this position.

To examine the transforming potential of RAC1(N92I), we infected mouse 3T3 fibroblasts and MCF10A human mammary epithelial cells (15) with a retrovirus encoding wild-type or N92I mutant form of human RAC1 and then seeded the cells in soft agar for evaluation of anchorage-independent growth. Neither 3T3 nor MCF10A cells expressing wild-type RAC1 grew in soft agar (Fig. 1*A*), indicating the lack of transforming potential of RAC1. In contrast, the cells expressing RAC1(N92I) readily grew in soft agar (Fig. 1*A*), showing that this RAC1 mutant confers the property of anchorage-independent growth on both 3T3 and MCF10A cells. We also confirmed the transforming potential of an artificial mutant of RAC1, RAC1(G12V) (8),

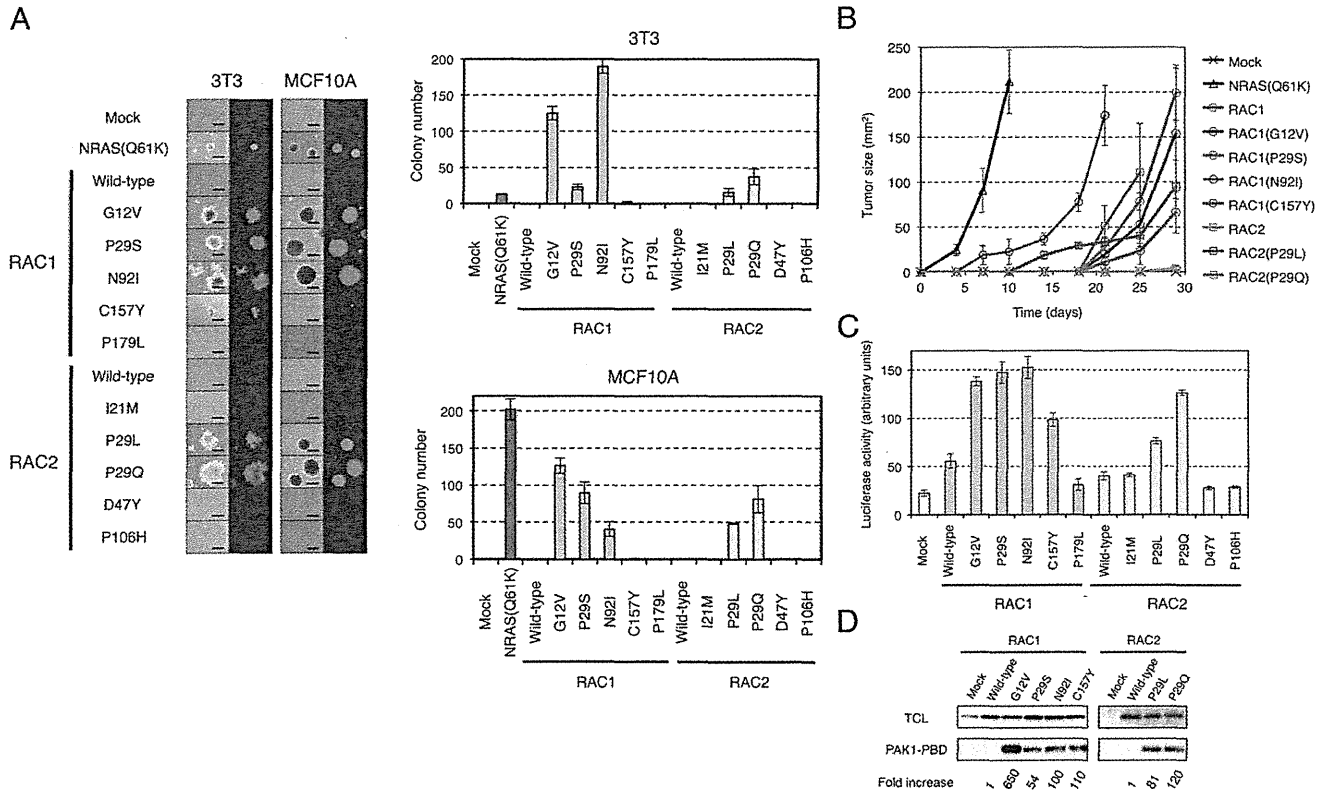

Fig. 1. Transforming potential of RAC1 and RAC2 mutants. (*A*) 3T3 or MCF10A cells were infected with recombinant retroviruses encoding enhanced green fluorescent protein (EGFP) as well as wild-type or mutant forms of RAC1 or RAC2 and were then assayed for anchorage-independent growth in vitro under the presence of 10% (vol/vol) FBS. After 14 d (3T3) or 20 d (MCF10A) of culture, the cells were stained with crystal violet and examined by conventional microscopy (*Left*: left image of each pair), and they were monitored for EGFP expression by fluorescence microscopy (*Left*: right image of each pair). (Scale bars, 0.5 mm.) The numbers of cell colonies were also determined as means ± SD from three independent experiments (*Right*). (*B*) 3T3 cells expressing wild-type or mutant forms of RAC1 or RAC2 were injected s.c. into the shoulder of nude mice, and the size of the resulting tumors [(length × width)/2] was determined at the indicated times thereafter. Tumor size for 3T3 expressing NRAS(Q61K) was similarly monitored. Data are means ± SD for tumors at four injection sites. (*C*) HEK293T cells were transfected with expression vectors for wild-type or mutant forms of RAC1 or RAC2 together with the SRE.L reporter plasmid and pGL-TK. The activity of firefly luciferase in cell lysates was then measured and normalized by that of *Renilla* luciferase. Data are means ± SD from three independent experiments. (*D*) Lysates of 3T3 cells expressing wild-type or mutant forms of RAC1 or RAC2 were subjected to a pull-down assay with PAK1-PBD. The precipitated proteins as well as the total cell lysates were then subjected to immunoblot analysis with antibodies to RAC1 or to RAC2. The relative amounts of pulled-down RAC proteins compared with their corresponding expression levels in total cell lysate were normalized to that of wild-type RAC1 (for the RAC1 mutants) or RAC2 (for the RAC2 mutants) and are shown at the bottom.

which harbors an amino acid substitution corresponding to that of the oncogenic G12V mutant form of RAS proteins.

Other Transforming Mutations of RAC1 and RAC2. We next searched for other transforming mutations of RAC proteins. Human RAC1, RAC2 (GenBank accession no. NM_002872.3), and RAC3 (GenBank accession no. NM_005052.2) cDNAs were isolated from 40 cancer cell lines (Table S2), and their nucleotide sequences were determined by Sanger sequencing, resulting in the discovery of RAC1(P29S), RAC2(P29Q), and RAC2(P29L) in the breast cancer cell line MDA-MB-157, the CML cell line KCL-22, and the breast cancer cell line HCC1143, respectively (Fig. S1 and Table S3). Further searching for *RAC1*, *RAC2*, and *RAC3* mutations in the COSMIC database of cancer genome mutations (Release V59; http://cancer.sanger.ac.uk/cancergenome/projects/cosmic) revealed various amino acid substitutions detected in human tumors, namely RAC1(P29S), RAC1(C157Y), RAC1(P179L), RAC2(I21M), RAC2(P29L), RAC2(D47Y), and RAC2(P106H) (Table S3). Importantly, all of these *RAC1* and *RAC2* mutations identified in clinical specimens were confirmed to be somatic, given that the corresponding mutations were absent in the genome of paired normal cells.

To examine the transforming potential of these various RAC1 and RAC2 mutants, we expressed each protein in 3T3 and MCF10A cells and evaluated anchorage-independent growth. Whereas the wild-type form of RAC2 did not transform 3T3 or MCF10A cells, growth in soft agar was apparent for 3T3 cells expressing RAC1 (P29S), RAC1(C157Y), RAC2(P29L), or RAC2(P29Q), but not for those expressing RAC1(P179L), RAC2(I21M), RAC2(D47Y), or RAC2(P106H) (Fig. 1*A*). Of interest, colony number in the assay varied substantially in a manner dependent on the type of amino acid substitution as well as on cell type. RAC1(C157Y), for example, yielded fewer colonies in soft agar compared with the other transforming mutants. Furthermore, RAC1(P29S), which was identified in a breast cancer cell line, generated a larger number of colonies with MCF10A cells than with 3T3 cells. Conversely, RAC1(N92I), which was identified in a fibrosarcoma cell line, yielded a larger number of colonies with 3T3 cells than with MCF10A cells. The oncogenic activity of RAC1(P29S), RAC1 (N92I), RAC1(C157Y), RAC2(P29L), and RAC2(P29Q) mutants was further confirmed with a tumorigenicity assay in nude mice (Fig. 1*B*), with the activity of RAC1(N92I) being the most pronounced with regard to the transformation of 3T3 cells in this assay.

The colony number in soft agar for 3T3 cells expressing NRAS (Q61K) was fewer than that for the cells expressing oncogenic RAC1 or RAC2 mutants (Fig. 1*A*), whereas expression of these small GTPases was readily confirmed in 3T3 (Fig. S2). Interestingly, s.c. tumors from the same 3T3 cells expressing NRAS(Q61K) grew more rapidly than tumors expressing the RAC1/RAC2 mutants (Fig. 1*B*), indicating that the measured intensity of the transforming potential of GTPases may vary in a dependent manner on assay systems.

To examine whether such oncogenic potential is linked directly to the activation of RAC1 or RAC2, we investigated the activity of the mutant proteins with the use of a luciferase reporter plasmid that selectively responds to intracellular signaling evoked by RHO family GTPases (16). In concordance with the data from the soft agar and tumorigenicity assays, only the transforming mutants of RAC1 and RAC2 yielded a substantial level of luciferase activity in transfected HEK293T cells (Fig. 1*C*).

Activated RAC1 or RAC2 would be expected to be loaded with GTP. We therefore examined the GTP-binding status of the RAC1 and RAC2 oncoproteins with the use of a pull-down assay based on the p21-binding domain (PBD) of PAK1. All of the transforming RAC1 and RAC2 mutants were found to exist preferentially in the GTP-bound state (Fig. 1*D*), indicative of their constitutive activation. Furthermore, these RAC1 and RAC2 mutants induced marked reorganization of the actin cytoskeleton in 3T3 cells, resulting in the accumulation of polymerized actin in ruffles at the plasma membrane (Fig. 2).

RAC1 and RAC2 as Therapeutic Targets. Given that NRAS(Q61K) is also known to transform 3T3 cells (17) (Fig. 1*A*), our data show that HT1080 cells harbor two independent oncogenic GTPases. We therefore examined whether RAC1(N92I) or NRAS(Q61K) is the principal growth driver in this sarcoma cell line. Among several small interfering RNAs (siRNAs) designed to attenuate the expression of RAC1 or NRAS, we selected two independent siRNAs that specifically target each mRNA (Fig. 3*A*). Whereas transfection of HT1080 cells with either NRAS siRNA resulted in a moderate inhibition of cell proliferation under the presence of 10% (vol/vol) FBS, that with either RAC1 siRNA almost blocked cell growth (Fig. 3*B*). Transfection with an NRAS siRNA in addition to either RAC1 siRNA did not result in an additional effect on cell proliferation (Fig. 3*B*). Similar data were observed in a culture with 1% (vol/vol) FBS (Fig. S3*A*) or under FBS-free conditions (Fig. S3*B*). To further examine the effects of silencing RAC1/NRAS, we quantitated cell cycle distribution of HT1080 transfected with siRNAs against either RAC1 or NRAS. As shown in Fig. S4*A*, DNA synthesis was equally suppressed by the knockdown of RAC1 or NRAS. Interestingly, however, CASP3/CASP7 activity (a surrogate marker for apoptosis) was markedly induced only by RAC1 depletion (Fig. S4*B*). Therefore, RAC proteins are likely to provide RAS-independent cell survival

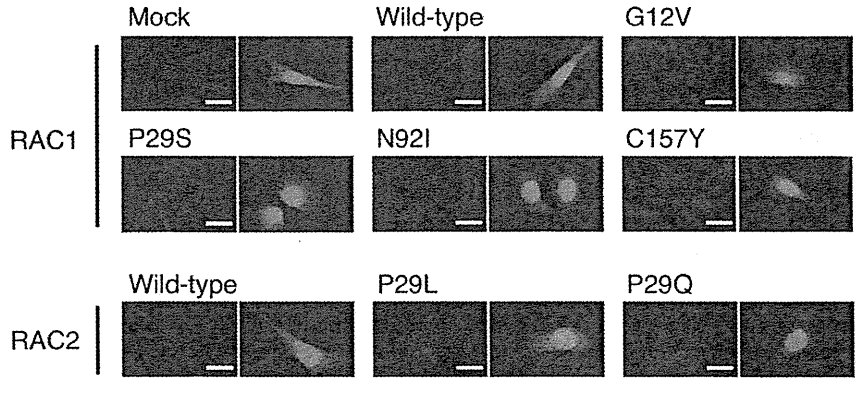

Fig. 2. Actin reorganization induced by the RAC1/RAC2 mutants. 3T3 cells infected with retroviruses encoding enhanced green fluorescent protein (EGFP) as well as wild-type or mutant forms of RAC1 or RAC2 were stained with Alexa Fluor 594-labeled phalloidin to visualize actin organization (*Left* image of each pair). The same cells were also examined for EGFP fluorescence (*Right* image of each pair). (Scale bars, 20 μm.)

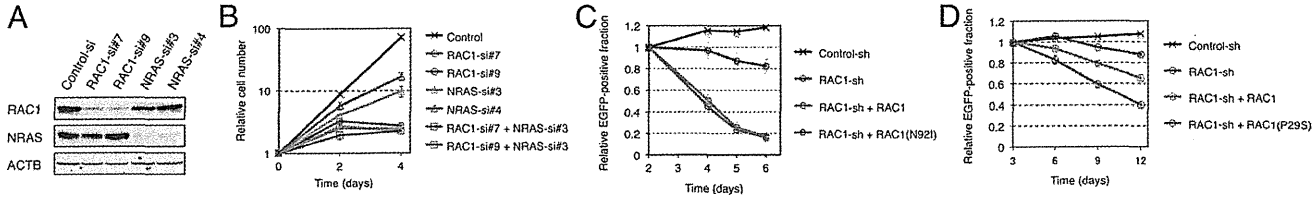

Fig. 3. Oncogenic RAC proteins as therapeutic targets. (*A*) HT1080 cells were transfected with control, RAC1, or NRAS siRNAs; lysed; and subjected to immunoblot analysis with antibodies to RAC1, NRAS, or ACTB (loading control). (*B*) HT1080 cells were transfected with control, RAC1, or NRAS siRNAs, as indicated, and cultured under the presence of 10% (vol/vol) FBS. Cell number was counted at the indicated times after the onset of transfection. Data are means ± SD from three independent experiments. (*C*) HT1080 cells were infected with a retrovirus encoding green fluorescent protein (EGFP) as well as a control or RAC1 shRNA. They were also infected with a retrovirus encoding shRNA-resistant wild-type RAC1 or RAC1(N92I), as indicated. The number of EGFP-positive cells was determined by flow cytometry after culture of the cells for the indicated times, and the size of the EGFP-positive fraction relative to that at 2 d was calculated. Data are means ± SD from three independent experiments. (*D*) MDA-MB-157 cells were infected with a retrovirus encoding EGFP as well as a control or RAC1 shRNA. They were also infected with a retrovirus encoding shRNA-resistant wild-type RAC1 or RAC1(P29S), as indicated. The number of EGFP-positive cells was determined by flow cytometry after culture of the cells for the indicated times, and the size of the EGFP-positive fraction relative to that at 3 d was calculated. Data are means ± SD from three independent experiments.

signals, which is supported by the fact that, even under FBS-free conditions, RAC1 depletion has more antiproliferative effects in HT1080 than NRAS depletion (Fig. S3*B*). These data show that active RAC1 may be the essential growth driver in HT1080 cells and is therefore a potential therapeutic target. Furthermore, our data suggest that oncogenic RAS proteins may require additional transforming hits to give rise to full-blown cancer.

We next infected HT1080 cells with a retrovirus expressing a short hairpin RNA (shRNA) targeted to RAC1 mRNA. Expression of the RAC1 shRNA markedly suppressed cell growth, whereas restoration of shRNA-resistant RAC1(N92I) expression reversed this effect (Fig. 3*C* and Fig. S5), showing that the effect of the RAC1 shRNA was not an off-target artifact. Forced expression of shRNA-resistant wild-type RAC1 failed to reverse the inhibitory effect of the RAC1 shRNA on cell growth, indicating that growth suppression by the shRNA was due to depletion of the N92I mutant, not to that of the wild-type protein. We performed similar experiments with the breast cancer cell line MDA-MB-157, which harbors RAC1(P29S). Again, the RAC1 shRNA inhibited cell growth, and this effect was reversed to a larger extent by restoration of the expression of shRNA-resistant RAC1(P29S) than by forced expression of the wild-type protein (Fig. 3*D* and Fig. S5).

RAC1(P29S), RAC1(N92I), and RAC1(C157Y) Are Rapid-Cycling Mutants. Oncogenic mutations at G12, G13, or Q61 of RAS proteins found in human tumors reduce the intrinsic GTPase activity of these

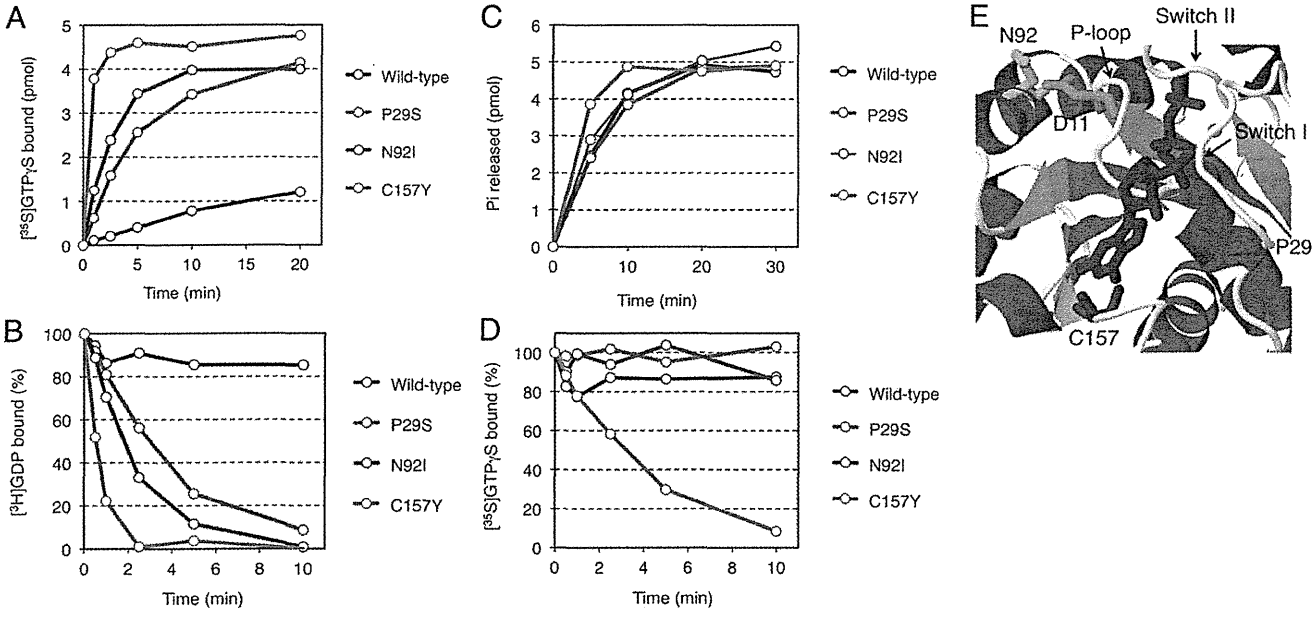

Fig. 4. Biochemical properties of RAC1 mutants. (*A*) Bacterially expressed and purified proteins of the wild-type, P29S, N92I, or C157Y mutant of RAC1 (5 pmol each) were incubated with [^{35}S]GTPγS in the presence of 0.8 mM Mg^{2+}, and the amounts of [^{35}S]GTPγS-bound proteins were determined at the indicated times. (*B*) [^{3}H]GDP dissociation from [^{3}H]GDP-bound RAC1 proteins was initiated by the addition of unlabeled GTPγS in the presence of 0.8 mM Mg^{2+}, and the amounts of [^{3}H]GDP-bound proteins were determined at the indicated times. (*C*) RAC1 proteins were preloaded with [γ^{32}P] GTP, and then GTP hydrolysis reactions were initiated by the addition of unlabeled GTP in the presence of 0.8 mM Mg^{2+}. P_i released from the proteins was isolated and measured at the indicated times. (*D*) [^{35}S]GTPγS dissociation from [^{35}S]GTPγS-bound RAC1 proteins was initiated by the addition of unlabeled GTPγS in the presence of 0.8 mM Mg^{2+}, and the amounts of [^{35}S]GTPγS-bound proteins were determined at the indicated times. (*E*) Schematic representation of the structure of the GTP-binding pocket of human RAC1 (ID 1mh1 in the Protein Data Bank; www.pdb.org) with α-helices and β-sheets shown in magenta and orange, respectively. The GTP analog guanosine 5′-(β,γ-imido)-triphosphate (GppNp) and Mg^{2+} are depicted in red and green, respectively. D11, P29, N92, and C157 amino acid residues are in orange, blue, yellow and purple, respectively. The positions of switch I and switch II regions and the P-loop are also indicated.

proteins and thereby maintain them in the GTP-bound state (18, 19). On the other hand, an artificial F28L substitution in HRAS or the RHO family protein Cdc42Hs was shown to confer constitutive activity by accelerating the transition from the GDP-bound to the GTP-bound state without the involvement of an exogenous guanine nucleotide exchange factor (GEF) (20, 21).

To determine how transforming mutations of RAC1 results in constitutive activation of these proteins, we examined their affinity for GTP and GDP. Compared with wild-type RAC1, all of RAC1(P29S), RAC1(N92I), and RAC1(C157Y) was found to bind GTPγS (nonhydrolyzable GTP analog) rapidly in vitro, even without the addition of a GEF protein (Fig. 4*A*). Likewise, the dissociation of GDP from the mutant forms of RAC1 was greatly accelerated (Fig. 4*B*). On the other hand, the intrinsic GTPase activity of these mutants was similar to (for P29S and N92I) or slightly higher (for C157Y) than that of the wild-type protein (Fig. 4*C*). These data thus indicated that, in contrast to transforming RAS mutants associated with human cancer, RAC1 (P29S), RAC1(N92I), and RAC1(C157Y) are fast-cycling mutants, for which the probability of being in the GTP-bound state is increased as the result of an increased rate of GDP dissociation, rather than as the result of a loss of GTPase activity.

Interestingly, dissociation of GTPγS was also accelerated only for RAC1(C157Y), but not for the wild-type, P29S, or N92I form of RAC1 (Fig. 4*D*). Thus, RAC1(C157Y) is a unique mutant in that both association and dissociation for GTP are accelerated, which may provide the molecular basis for its modest transforming potential compared with that of RAC1(P29S) or RAC1 (N92I) (Fig. 1).

In the 3D structure of RAC1 (Fig. 4*E*), P29 is located in the switch I region, whereas C157 is positioned adjacent to the guanine ring of bound GTP. Substitution of these residues would thus likely affect the affinity of the protein for GDP or GTP (Fig. S6), a phenomenon that has been demonstrated recently for RAC1 (P29S) (22). In contrast, N92 is located distant from the binding pocket for GDP/GTP, and so the structural mechanism by which the N92I substitution renders RAC1 constitutively active remains elusive (Fig. 4*E* and Fig. S6). Residue N92 is located close to D11 in the P-loop of RAC1, however (Fig. 4*E* and Fig. S7), and substitution with isoleucine at this position would abolish the interaction between the amino group of N92 and the carboxyl group of D11. It is thus possible that the N92I mutation affects the binding of GDP/GTP through an effect on the P-loop.

Discussion

We have here demonstrated the transforming potential of mutated RAC proteins. Our analysis of cell lines resulted in the identification of transforming mutants of RAC1 and RAC2, namely RAC1(N92I) and RAC2(P29Q), and we also revealed the transforming potential of the RAC1(P29S), RAC1(C157Y), and RAC2(P29L) mutants deposited the COSMIC database of cancer genome mutations (Release V59; http://cancer.sanger.ac.uk/cancergenome/projects/cosmic) (Table S3). In contrast, the soft agar assay did not reveal a transforming potential of the RAC1(P179L), RAC2(I21M), RAC2(D47Y), or RAC2(P106H) mutants found in the database, suggesting a possibility that they are "passenger mutations." It may also be possible, however, that these mutants may still contribute to cancer development by modifying tumor properties (such as metastasis ability), given that they were somatically acquired and clonally selected in cancer.

An important finding of our study was that the oncogenic effects of RAC1(N92I) may be more pronounced than those of NRAS(Q61K), at least with regard to survival signals in HT1080 cells (Fig. 3*B*). It should be noted, however, that HT1080 expresses RAC1 almost exclusively among the RAC family proteins, whereas HRAS and KRAS are weakly expressed in addition to NRAS (Fig. S8). It is thus possible that the effects of NRAS knockdown in Fig. 3*B* may be partly complemented by the residual HRAS/KRAS proteins.

Paterson et al. previously isolated NRAS-attenuated subclones of HT1080 after treatment with an alkylating reagent (*N*-methyl-*N*′-nitro-*N*-nitrosoguanidine) and a subsequent culture with 5-fluorodeoxyuridine and 1-β-D-arabinofuranosylcytosine (23). Such subclones had a flat cell shape and a reduced ability for anchorage-independent growth. Likewise, we noted that transfection with NRAS siRNAs renders HT1080 a flatter shape (Fig. S9). As demonstrated in Fig. 3*B* and by Paterson et al. (23), however, such NRAS-depleted HT1080 was still viable and kept proliferation in vitro, suggesting the presence of other oncogene(s) in addition to NRAS(Q61K). Therefore, NRAS(Q61K) and RAC1(N92I) are likely to cooperate to fully transform this fibrosarcoma.

Regarding the coexistence of mutations within RAC family proteins and RAS-RAF-MAPK proteins, two studies independently reported recurrent P29S mutation of RAC1 in melanoma during the preparation of this article (22, 24). Of note, BRAF (V600E) was also detected in four of six and in two of seven of the RAC mutation-positive melanomas, respectively. These observations, together with our findings with HT1080 cells, thus indicate that activating mutations of RAC1 and those of the RAS-RAF–signaling pathway are not mutually exclusive.

Members of the RAC subfamily of GTPases show a high level of sequence identity in humans. The amino acid sequence of RAC1 is thus 92% identical to that of RAC2 or RAC3. Furthermore, all of the amino acid residues of RAC1 or RAC2 found to be mutated in cancer (Table S3) are completely conserved among RAC1, RAC2, and RAC3. Thus, transforming RAC3 mutants with similar nonsynonymous mutations may also exist in human cancer, although such mutations were not detected in the current screening. Of interest, none of the frequent mutation sites in RAS family proteins (G12, G13, and Q61) were found to be affected in RAC1 or RAC2, although an artificial G12V mutant of RAC1 did manifest constitutive GTP loading and transforming potential. Given that RAC proteins perform intracellular functions (such as orchestration of the actin cytoskeleton) that are distinct from those of RAS family members, RAC-driven activation of specific intracellular pathways may be advantageous for cancer development in vivo.

Given that we detected activation mutations of RAC1 or RAC2 in cell lines from sarcoma (HT1080), triple-negative breast cancer (MDA-MB-157 and HCC1143), and the blast crisis stage of CML (KCL-22), we performed deep sequencing of *RAC1*, *RAC2*, and *RAC3* cDNAs with GAIIx for specimens of triple-negative breast cancer (n = 66), of *RAC1* and *RAC2* cDNAs for specimens of CML in blast crisis (n = 43), and of *BCR-ABL1*–positive acute lymphoblastic leukemia (n = 31), as well as of *RAC1* cDNAs for specimens of sarcoma (n = 53). We failed, however, to detect any nonsynonymous mutations among these RAC cDNAs.

Our results have shown that RAC proteins have the potential to become oncogenic through amino acid substitution in a wide array of cancers. Although such RAC mutations may occur at a low frequency, the recent studies of Krauthammer et al. (22) and Hodis et al. (24) suggest that they may be enriched in melanoma (~5%). Importantly, given that HT1080 cells are highly addicted to the increased activity of RAC1(N92I), the targeting of oncogenic RAC proteins or their downstream effectors with small compounds or RNAi may prove to be an effective approach to the treatment of cancer harboring such oncoproteins.

Materials and Methods

The human fibrosarcoma cell line HT1080 was obtained from American Type Culture Collection, and subjected to deep sequencing with GAIIx. Recombinant retrovirus expressing the wild-type or mutant forms of RAC1 or RAC2 was used to infect mouse 3T3 fibroblasts to examine its transforming potential. Detailed information for cDNA resequencing, transformation assays, biochemical analysis of RAC proteins, and RNAi are detailed in *SI Materials and Methods*.

ACKNOWLEDGMENTS. This study was supported in part by a grant for Research on Human Genome Tailor-Made from the Ministry of Health, Labor, and Welfare of Japan; Grants-in-Aid for Scientific Research (B) from the Japan Society for the Promotion of Science; and grants from The Yasuda Medical Foundation, The Sagawa Foundation for Promotion of Cancer Research, and The Mitsubishi Foundation.

1. Druker BJ, et al.; IRIS Investigators (2006) Five-year follow-up of patients receiving imatinib for chronic myeloid leukemia. *N Engl J Med* 355(23):2408–2417.
2. Soda M, et al. (2007) Identification of the transforming *EML4-ALK* fusion gene in non-small-cell lung cancer. *Nature* 448(7153):561–566.
3. Shaw AT, et al. (2011) Effect of crizotinib on overall survival in patients with advanced non-small-cell lung cancer harbouring ALK gene rearrangement: A retrospective analysis. *Lancet Oncol* 12(11):1004–1012.
4. Colicelli J (2004) Human RAS superfamily proteins and related GTPases. *Sci STKE* 2004 (250):RE13.
5. Cox AD, Der CJ (2010) Ras history: The saga continues. *Small GTPases* 1(1):2–27.
6. Jaffee EM, Hruban RH, Canto M, Kern SE (2002) Focus on pancreas cancer. *Cancer Cell* 2(1):25–28.
7. Wertheimer E, et al. (2012) Rac signaling in breast cancer: A tale of GEFs and GAPs. *Cell Signal* 24(2):353–362.
8. Ridley AJ, Paterson HF, Johnston CL, Diekmann D, Hall A (1992) The small GTP-binding protein rac regulates growth factor-induced membrane ruffling. *Cell* 70(3):401–410.
9. Qiu RG, Chen J, Kirn D, McCormick F, Symons M (1995) An essential role for Rac in Ras transformation. *Nature* 374(6521):457–459.
10. Senger DL, et al. (2002) Suppression of Rac activity induces apoptosis of human glioma cells but not normal human astrocytes. *Cancer Res* 62(7):2131–2140.
11. Thomas EK, et al. (2007) Rac guanosine triphosphatases represent integrating molecular therapeutic targets for BCR-ABL-induced myeloproliferative disease. *Cancer Cell* 12(5):467–478.
12. Rasheed S, Nelson-Rees WA, Toth EM, Arnstein P, Gardner MB (1974) Characterization of a newly derived human sarcoma cell line (HT-1080). *Cancer* 33(4):1027–1033.
13. Ueno T, et al. (2012) High-throughput resequencing of target-captured cDNA in cancer cells. *Cancer Sci* 103(1):131–135.
14. Hall A, Marshall CJ, Spurr NK, Weiss RA (1983) Identification of transforming gene in two human sarcoma cell lines as a new member of the ras gene family located on chromosome 1. *Nature* 303(5916):396–400.
15. Debnath J, Muthuswamy SK, Brugge JS (2003) Morphogenesis and oncogenesis of MCF-10A mammary epithelial acini grown in three-dimensional basement membrane cultures. *Methods* 30(3):256–268.
16. Hill CS, Wynne J, Treisman R (1995) The Rho family GTPases RhoA, Rac1, and CDC42Hs regulate transcriptional activation by SRF. *Cell* 81(7):1159–1170.
17. Marshall CJ, Hall A, Weiss RA (1982) A transforming gene present in human sarcoma cell lines. *Nature* 299(5879):171–173.
18. Adari H, Lowy DR, Willumsen BM, Der CJ, McCormick F (1988) Guanosine triphosphatase activating protein (GAP) interacts with the p21 ras effector binding domain. *Science* 240(4851):518–521.
19. Calés C, Hancock JF, Marshall CJ, Hall A (1988) The cytoplasmic protein GAP is implicated as the target for regulation by the ras gene product. *Nature* 332(6164): 548–551.
20. Reinstein J, Schlichting I, Frech M, Goody RS, Wittinghofer A (1991) p21 with a phenylalanine 28——leucine mutation reacts normally with the GTPase activating protein GAP but nevertheless has transforming properties. *J Biol Chem* 266(26): 17700–17706.
21. Lin R, Bagrodia S, Cerione R, Manor D (1997) A novel Cdc42Hs mutant induces cellular transformation. *Curr Biol* 7(10):794–797.
22. Krauthammer M, et al. (2012) Exome sequencing identifies recurrent somatic RAC1 mutations in melanoma. *Nat Genet* 44(9):1006–1014.
23. Paterson H, et al. (1987) Activated N-ras controls the transformed phenotype of HT1080 human fibrosarcoma cells. *Cell* 51(5):803–812.
24. Hodis E, et al. (2012) A landscape of driver mutations in melanoma. *Cell* 150(2): 251–263.

Published OnlineFirst May 2, 2012; DOI:10.1158/1078-0432.CCR-11-2972

Clinical Cancer Research

Cancer Therapy: Preclinical

Paracrine Receptor Activation by Microenvironment Triggers Bypass Survival Signals and ALK Inhibitor Resistance in EML4-ALK Lung Cancer Cells

Tadaaki Yamada[1], Shinji Takeuchi[1], Junya Nakade[1], Kenji Kita[1], Takayuki Nakagawa[1,2], Shigeki Nanjo[1], Takahiro Nakamura[3], Kunio Matsumoto[3], Manabu Soda[4], Hiroyuki Mano[4], Toshimitsu Uenaka[2], and Seiji Yano[1]

Abstract

Purpose: Cancer cell microenvironments, including host cells, can critically affect cancer cell behaviors, including drug sensitivity. Although crizotinib, a dual tyrosine kinase inhibitor (TKI) of ALK and Met, shows dramatic effect against *EML4-ALK* lung cancer cells, these cells can acquire resistance to crizotinib by several mechanisms, including ALK amplification and gatekeeper mutation. We determined whether microenvironmental factors trigger ALK inhibitor resistance in *EML4-ALK* lung cancer cells.

Experimental Design: We tested the effects of ligands produced by endothelial cells and fibroblasts, and the cells themselves, on the susceptibility of *EML4-ALK* lung cancer cell lines to crizotinib and TAE684, a selective ALK inhibitor active against cells with *ALK* amplification and gatekeeper mutations, both *in vitro* and *in vivo*.

Results: *EML4-ALK* lung cancer cells were highly sensitive to ALK inhibitors. EGF receptor (EGFR) ligands, such as EGF, TGF-α, and HB-EGF, activated EGFR and triggered resistance to crizotinib and TAE684 by transducing bypass survival signaling through Erk1/2 and Akt. Hepatocyte growth factor (HGF) activated Met/Gab1 and triggered resistance to TAE684, but not crizotinib, which inhibits Met. Endothelial cells and fibroblasts, which produce the EGFR ligands and HGF, respectively, decreased the sensitivity of *EML4-ALK* lung cancer cells to crizotinib and TAE684, respectively. EGFR-TKIs resensitized these cells to crizotinib and Met-TKI to TAE684 even in the presence of EGFR ligands and HGF, respectively.

Conclusions: Paracrine receptor activation by ligands from the microenvironment may trigger resistance to ALK inhibitors in *EML4-ALK* lung cancer cells, suggesting that receptor ligands from microenvironment may be additional targets during treatment with ALK inhibitors. *Clin Cancer Res; 18(13); 3592–602. ©2012 AACR.*

Introduction

ALK fusion with EML4 in non–small cell lung cancer (NSCLC) was first detected in 2007 (1), with 3% to 7% of unselected NSCLCs having this fusion gene (1–4). EML4-ALK lung cancer is more frequently observed in patients with adenocarcinoma than with other histologies, in young adults than in older patients, and in never-smokers or light smokers (<15 pack-years) than in heavier smokers (2, 3). ALK kinase inhibitors show dramatic effects against lung cancers with *EMK4-ALK in vitro* and *in vivo* (3, 4). In a phase I–II trial with crizotinib, a dual tyrosine kinase inhibitor (TKI) of ALK and Met, the overall response rate was 47 of 82 (57%) patients with *EML4-ALK*–positive tumors (5). However, almost all patients who show a marked response to ALK-TKIs acquire resistance to these agents after varying periods of time (6, 7). Secondary mutations, including the gatekeeper L1196M mutation and others (F1174L, C1156Y, G1202R, S1206Y, 1151-T-ins, and G1269A), *ALK* amplification, *KIT* amplification, and autophosphorylation of EGF receptor (EGFR), were shown to be responsible for acquired resistance to crizotinib in ALK-translocated cancers (6–10).

Selective ALK inhibitors, including TAE684 and CH5424802, have been reported active against *EML4-ALK* lung cancer cells with *ALK* amplification and secondary mutations. These cells, however, may develop resistance to this class of inhibitor, due to several mechanisms, including novel *ALK* mutations (L1152R, L1198P, and D1203N), coactivation of EGFR and ErbB2, and EGFR phosphorylation (3, 11, 12).

Authors' Affiliations: [1]Division of Medical Oncology, Cancer Research Institute, Kanazawa University, Kanazawa, Ishikawa; [2]Tsukuba Research Laboratories, Eisai co., ltd., Ibaraki; [3]Division of Tumor Dynamics and Regulation, Cancer Research Institute, Kanazawa University, Kanazawa, Ishikawa; and [4]Division of Functional Genomics, Jichi Medical University, Shimotsuke, Tochigi, Japan

Note: Supplementary data for this article are available at Clinical Cancer Research Online (http://clincancerres.aacrjournals.org/).

Corresponding Author: Seiji Yano, Division of Medical Oncology, Cancer Research Institute, Kanazawa University 13-1, Takara-machi, Kanazawa, Ishikawa 920-0934, Japan. Phone: 81-76-265-2794; Fax: 81-76-234-4524; E-mail: syano@staff.kanazawa-u.ac.jp

doi: 10.1158/1078-0432.CCR-11-2972

Published OnlineFirst May 2, 2012; DOI:10.1158/1078-0432.CCR-11-2972

Translational Relevance

Although crizotinib, a dual inhibitor of ALK and Met, shows dramatic effects against *EML4-ALK* lung cancer cells, these cells can acquire resistance by several mechanisms, including ALK amplification and gatekeeper mutation. Selective ALK inhibitors may overcome crizotinib resistance due to these mechanisms, but these cells may become resistant to these inhibitors.

We show here that EGF receptor ligands produced by endothelial cells can cause *EML4-ALK* lung cancer cells to become resistant to crizotinib and selective ALK inhibitors by triggering bypass survival signals. By contrast, hepatocyte growth factor produced by fibroblasts can induce resistance to selective ALK inhibitors, but not crizotinib. Because endothelial cells and fibroblasts are components of the microenvironment, our findings raise clinical questions about the class of ALK inhibitors more beneficial for *EML4-ALK* lung cancer patients. Moreover, our results provide a rationale for targeting receptor ligands in the microenvironment for more successful treatment with ALK inhibitors.

Most human cancers are composed of cancer cells that coexist with a variety of extracellular matrix components and cell types, including fibroblasts, endothelial cells, and immune cells, which collectively form the tumor microenvironment (13). This microenvironment can influence the growth, survival, invasiveness, metastatic ability, and drug sensitivity of cancer cells within these tumors (14). Paracrine signaling between cancer cells and host cells in the microenvironment, mediated by cytokines, chemokines, growth factors, and other signaling molecules, plays a critical role in tumor growth (15). As receptors for these factors, the EGFR family of receptors and Met are of particular interest in lung cancer (16). The EGFR family consists of at least 4 receptor tyrosine kinases, including EGFR (ErbB1), Her2/neu (ErbB2), HER3 (ErbB3), and HER4 (ErbB4). To date, 7 ligands for EGFR have been identified: EGF, TGF-α; heparin-binding EGF-like growth factor (HB-EGF); amphiregulin; betacellurin; epiregulin; and epigen (17). By contrast, Met is the only specific receptor for hepatocyte growth factor (HGF) and HGF binds only to Met (18). Many lung cancer cells express EGFR and Met, with these cells and others in their microenvironment expressing their ligands (19, 20), suggesting that these receptors and ligands modulate the sensitivity of cancer cells to molecular targeted drugs in their microenvironment. We previously showed that fibroblast-derived HGF induces EGFR-TKI resistance in *EGFR*-mutant lung cancer cells by activating Met and downstream pathways (21, 22). However, the role of the microenvironment in the sensitivity of EML4-ALK lung cancer cells to ALK-TKIs has not been determined. We therefore examined whether factors in the microenvironment of *EML4-ALK* lung cancer cells trigger their resistance to crizotinib and TAE684, a selective ALK inhibitor, as well as clarifying their underlying mechanisms of action.

Materials and Methods

Cell culture

The H2228 human lung adenocarcinoma cell line, with the EML4-ALK fusion protein variant3 (E6;A20), the umbilical vein endothelial cell line human umbilical vein endothelial cells (HUVEC) and the human bronchial epithelial cell line BEAS-2B, transformed with SV40 virus, were purchased from the American Type Culture Collection. The H3122 human lung adenocarcinoma cell line, with the EML4-ALK fusion protein variant1 (E13;A20), was kindly provided by Dr. Jeffrey A. Engelman of the Massachusetts General Hospital Cancer Center, Boston, MA (3). The MANA2 mouse lung adenocarcinoma cell line was established in Jichi Medical University from a tumor nodule developed in a transgenic mouse expressing *EML4-ALK* variant 1 (E13;A20) (23). The MRC-5 and IMR-90 lung embryonic fibroblast cell lines were obtained from RIKEN Cell Bank. The human dermal microvessel endothelial cell line HMVEC was purchased from Kurabo. The monocytic leukemia cell line U937 was purchased from Health Science Research Resources Bank. H2228 cells were cultured in RPMI-1640 medium, MANA2 cells were cultured in DMEM/F12+GlutaMAX-1, and MRC-5 (P 25–30) cells were cultured in Dulbecco's modified Eagle's medium (DMEM) medium, supplemented with 5% fetal bovine serum, penicillin (100 U/mL), and streptomycin (50 μg/mL), in a humidified CO_2 incubator at 37°C. HMVECs and HUVECs were maintained in HuMedia-MvG with growth supplements (Kurabo) and used for *in vitro* assays at passages 2 to 5 and 2 to 4, respectively. BEAS-2B cells were maintained in LHC9/RPMI-1640 medium, as described (24), and used for *in vitro* assays at passages 42 to 46. Macrophage differentiation of U937 cells was induced by incubation in RPMI-1640 medium containing 10 ng/mL phorbol 12-myristate 13-acetate (Sigma Chemical Co.; ref. 25) for 5 days, with floating cells removed by rinsing with PBS, as described (26). Differentiated U937 cells (PMA-U937 cells) attached to the dishes were used for *in vitro* assays at passages 6 to 8. All cells were passaged for less than 3 months before renewal from frozen, early-passage stocks obtained from the indicated sources. Cells were regularly screened for *Mycoplasma* using a MycoAlert *Mycoplasma* Detection Kit (Lonza).

Reagents

TAE684, crizotinib, and WZ4002 were purchased from Seleck Chemicals. Erlotinib hydrochloride was obtained from Chugai Pharmaceutical Co., Ltd. The anti-human EGFR antibody cetuximab was obtained from Merck Serono. E7050 was synthesized by Eizai Co., Ltd. (27). Goat anti-human HGF antibody, control goat IgG, recombinant EGF, TGF-α, HB-EGF, IGF-1, and PDGF-AA were purchased from R&D Systems. Recombinant HGF was prepared as described (28).

Published OnlineFirst May 2, 2012; DOI:10.1158/1078-0432.CCR-11-2972

Cell growth assay

Cell proliferation was measured using the MTTdye reduction method (17). Tumor cells at 80% confluence were harvested, seeded at 2×10^3 cells per well in 96-well plates, and incubated in appropriate medium for 24 hours. Several concentrations of TAE684, crizotinib, erlotinib, WZ4002, E7050, cetuximab, anti-HGF antibody, and/or EGF, TGF-α, HB-EGF, IGF-1, PDGF-AA, and HGF were added to each well, and incubation was continued for a further 72 hours. To each well was added 50 μL MTT (2 mg/mL; Sigma), followed by incubation for 2 hours at 37°C. The media were removed and the dark blue crystals in each well were dissolved in 100 μL of dimethyl sulfoxide (DMSO). Absorbance was measured with an MTP-120 Microplate reader (Corona Electric) at test and reference wavelengths of 550 and 630 nm, respectively. The percentage growth was calculated relative to untreated controls. Each assay was carried out at least in triplicate, with results based on 3 independent experiments.

Apoptosis assay

H2228 and H3122 cells (3×10^3 cells) were seeded in 96-well, white-walled plates and incubated overnight. The cells were treated with crizotinib (1 μmol/L) or vehicle (DMSO) for 48 hours. Cellular apoptosis was determined by measuring caspase-3/7 activity using a luminometric Caspase-Glo 3/7 assay (Promega) according to the manufacturer's protocol, with luminescence intensity measured using a Fluoroskan Ascent FL plate reader (Thermo Scientific). Cellular apoptosis was expressed relative to DMSO-treated control cells.

RNA interference

Duplexed Stealth RNAi (Invitrogen) against *EGFR*, *Met*, *ErbB3*, *Gab1*, *ALK*, and Stealth RNAi-negative control low GC Duplex #3 (Invitrogen) were used for RNA interference (RNAi) assays. Briefly, aliquots of 1×10^5 cells in 2 mL of antibiotic-free medium were plated into each well of a 6-well plate and incubated at 37°C for 24 hours. The cells were transfected with siRNA (250 pmol) or scrambled RNA using Lipofectamine 2000 (5 μL) in accordance with the manufacturer's instructions (Invitrogen). After 24 hours, the cells were washed twice with PBS and incubated with or without crizotinib (100 nmol/L), TAE684 (100 nmol/L), recombinant human EGF (100 ng/mL), TGF-α (100 ng/mL), HB-EGF (10 ng/mL), or HGF (50 ng/mL) for an additional 48 hours in antibiotic-containing medium. These tumor cells were then used for cell proliferation assays, with *EGFR*, *Met*, *ErbB3*, *Gab1*, and *ALK* knockdowns (#1, #2) confirmed by Western blotting.

The siRNA target sequences were as follows: *EGFR*, 5′-CGGAATAGGTATTGGTGAATTTAAA-3′ and 5′-UUUAAAUUCACCAAUACCUAUUCCG-3′, *Met*, 5′-UCCAGAAGAUCAGUUUCCUAAUUCA-3′ and 5′-UGAAUUAGGAAACUGAUCUUCUGGA-3′, *ErbB3*, 5′-GGCCAUGAAUGAAUUCUCUACUCUA-3′ and 5′-UAGAGUAGAGAAUUCAUUCAUGGCC-3′, *Gab1*, 5′-UAGAGUAGCAGAGGAUGAAUCUGCC-3′ and 5′-GGCAGAUUCAUCCUCUGCUACUCUA-3′, *ALK #1*, 5′-UCAUUAUCCGGUAUACAGGCCCAGG-3′ and 5′-CCUGGGCCUGUAUACCGGAUAAUGA-3′, and ALK #2, 5′-AAAGCUGCACUCCAGACCAUAUCGG-3′ and 5′-CCGAUAUGGUCUGGAGUGCAGCUUU-3′. Each assay was carried out at least in triplicate, with 3 independent experiments conducted.

Western blotting

SDS polyacrylamide gels (Bio-Rad) were loaded with 40 μg total protein per lane; following electrophoresis, the proteins were transferred onto polyvinylidene difluoride membranes (Bio-Rad), which were incubated with Blocking One (Nacalai Tesque) for 1 hour at room temperature, followed by overnight incubation at 4°C with anti-ALK (C26G7), anti–phospho-ALK (Tyr1604), anti–phospho-EGFR (Tyr1068), anti-STAT-3(79D7), anti–phospho-STAT-3 (Y705), anti-Akt, anti–phospho-Akt (Ser473), anti-ErbB4 (111B2), anti–phospho-ErbB4 (Tyr1284), anti-Met (25H2), anti–phospho-Met (Y1234/Y1235) (3D7), anti-Gab1 (#3232), anti-phospho-Gab1 (Tyr627) (C32H2), anti-ErbB3 (1B2), anti–phospho-ErbB3 (Tyr1289) (21D3), or anti-β-actin (13E5) antibodies (1:1,000 dilution each; Cell Signaling Technology), or with anti-human EGFR (1 μg/mL), anti-human/mouse/rat extracellular signal-regulated kinase (Erk)1/Erk2 (0.2 μg/mL), or anti-phospho-Erk1/Erk2 (T202/Y204) (0.1 μg/mL) antibodies (R&D Systems). After washing 3 times, the membranes were incubated for 1 hour at room temperature with secondary Ab (horseradish peroxidase–conjugated species-specific Ab). Immunoreactive bands were visualized with SuperSignal West Dura Extended Duration Substrate Enhanced Chemiluminescent Substrate (Pierce). Each experiment was carried out at least 3 times independently.

HGF, EGF, TGF-α, and HB-EGF production in cell culture supernatant

Cells (2×10^5) were cultured in 2 mL of RPMI-1640 or DMEM with 5% FBS for 24 hours. The cells were washed with PBS and incubated for 48 hours in RPMI-1640 or DMEM with 5% FBS. The culture medium was harvested and centrifuged, and the supernatant was stored at −70°C until analysis. HGF (Immunis HGF EIA; B-Bridge International), EGF, TGF-α, and HB-EGF (Quantikine ELISA kits; R&D Systems) were assayed by ELISA, in accordance with the manufacturer's procedures. All samples were run in triplicate. Color intensity was measured at 450 nm with a spectrophotometric plate reader. Growth factor concentrations were determined by comparison with standard curves. The detection limits for HGF, EGF, TGF-α, and HB-EGF were 0.1 ng/mL, 3.9 pg/mL, 15.6 pg/mL, and 31.2 pg/mL, respectively.

Coculture of lung cancer cells with fibroblasts or endothelial cells

Cells were cocultured in Transwell Collagen-Coated chambers separated by an 8-μm (BD Biosciences, Erembodegem) or 3-μm (Corning Costar) pore size filter. Tumor cells (8×10^3 cells/800 μL) with or without TAE684

Published OnlineFirst May 2, 2012; DOI:10.1158/1078-0432.CCR-11-2972

(100 nmol/L) or crizotinib (100 nmol/L) in the lower chamber were cocultured with MRC-5 (1×10^4 cells/300 μL) or HMVEC (1×10^4 cells/300 μL) cells, with or without 2 hours of pretreatment with anti-human HGF antibody (2 μg/mL) or cetuximab (2 μg/mL) in the upper chamber for 72 hours. The upper chamber was then removed, 200 μL of MTT solution (2 mg/mL; Sigma) was added to each well and the cells were incubated for 2 hours at 37°C. The media were removed and the dark blue crystals in each well were dissolved in 400 μL of DMSO. Absorbance was measured with an MTP-120 Microplate reader (Corona Electric) at test and reference wavelengths of 550 and 630 nm, respectively. The percentage growth was measured relative to untreated controls. All samples were assayed at least in triplicate, with each experiment conducted 3 times independently.

Xenograft studies in SCID mice

Suspensions of H2228 cells (5×10^6), with or without MRC-5 cells (5×10^6), were injected subcutaneously into the backs of 5-week-old male severe combined immunodeficient (SCID) mice (Japan Clea). After 4 days (tumors diameter >4 mm), mice were randomly allocated into groups of 6 animals to receive TAE684 (1.25 mg/kg/d) or vehicle by oral gavage. Tumor size was measured with digital calipers, and tumor volume was calculated as 0.5 × length × (width)^2. All animal experiments complied with the Guidelines for the Institute for Experimental Animals, Kanazawa University Advanced Science Research Center (approval no. AP-081088).

HGF production in tumor tissues

Tumors obtained from SCID mice after 4 and 8 days were lysed in mammalian tissue lysis buffer containing a phosphatase and proteinase inhibitor cocktail (Sigma). HGF was quantitated by ELISA (Immunis HGF EIA; Institute of Immunology), with a detection limit of 0.1 ng/mL. All samples were assayed in triplicate.

Statistical analysis

Differences were analyzed by one-way ANOVA. All statistical analyses were carried out using GraphPad Prism Ver. 4.01 (GraphPad Software, Inc.). $P < 0.05$ was considered significant.

Results

HGF and/or EGFR ligands reduced the sensitivity of EML4-ALK lung cancer cells to ALK inhibitor *in vitro*

We first examined the sensitivity of human H2228, human H3122, and mouse MANA2 lung cancer cell lines, all containing EML4-ALK translocations, to the ALK inhibitors crizotinib and TAE684, and to various EGFR-TKIs. Human H2228 cells with *EML4-ALK* variant 3 (E6;A20) and H3122 cells with *EML4-ALK* variant 1 (E13;A20) were insensitive to the EGFR-TKIs erlotinib (a reversible EGFR-TKI) and WZ4002 (selective for mutant EGFR), but sensitive to the ALK-TKIs crizotinib and TAE684 (Fig. 1). MANA2 cells, established from lung tumors of an *EML4-ALK* variant 1 (E13;A20) transgenic mouse, were also sensitive to crizotinib and TAE684, although their viability was slightly inhibited by high concentrations (1 μmol/L) of EGFR-TKIs.

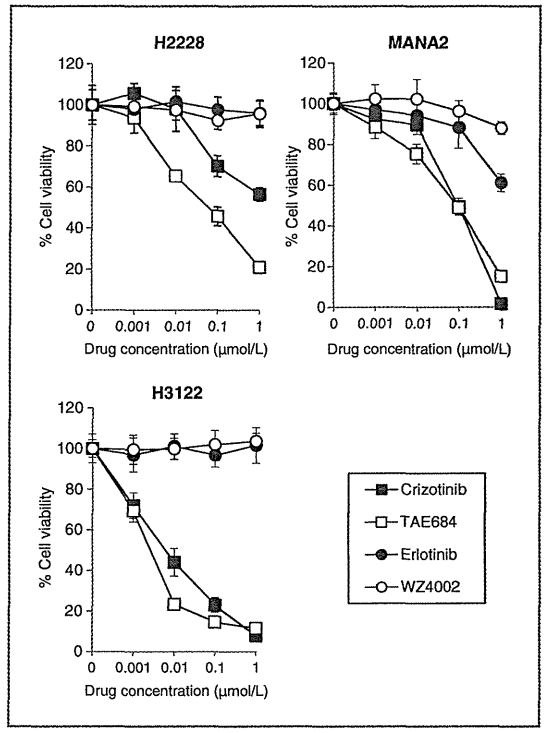

Figure 1. EML4-ALK lung cancer cells are highly sensitive to the ALK inhibitors, crizotinib, and TAE684. The sensitivity of EML4-ALK lung cancer cells, human H2228, human H3122, and mouse MANA2, to the ALK inhibitors, crizotinib, and TAE684 were determined by analyzing the effects of the EGFR-TKIs, erlotinib (reversible EGFR-TKI), and WZ4002 (mutant EGFR selective TKI). Tumor cell growth after 72 hours was measured by the MTT assay. Each sample was assayed in triplicate, with each experiment repeated at least 3 times independently.

Because several growth factors have been associated with poor patient prognosis and/or drug resistance in lung cancer, we explored the effect of EGFR ligands (EGF, TGF-α, and HB-EGF), IGF-1, PDGF-AA, and HGF on the sensitivity of *EML4-ALK* lung cancer cells to ALK inhibitors. In the absence of ALK inhibitors, these growth factors slightly increased the viability of H2228, H3122, and MANA2 cells. In H2228 cells, all 3 EGFR ligands reduced sensitivity to crizotinib in a dose-dependent manner, but IGF-1, PDGF-AA, and HGF failed to do so (Fig. 2, Supplementary Fig. S1). Interestingly, HGF, as well as the EGFR ligands, reduced sensitivity to TAE684, but IGF-1 and PDGF-AA failed to do so. Similar results were observed in H3122 and MANA2 cells. To further confirm the effect of these growth factors on specific ALK inhibition, we knocked down ALK using 2 different specific siRNAs in H2228 cells. Whereas H2228 cells were highly sensitive to *ALK*-specific siRNAs, EGFR ligands and HGF restored cell viability inhibited by ALK knockdown (Supplementary Fig. S2). When we

Published OnlineFirst May 2, 2012; DOI:10.1158/1078-0432.CCR-11-2972

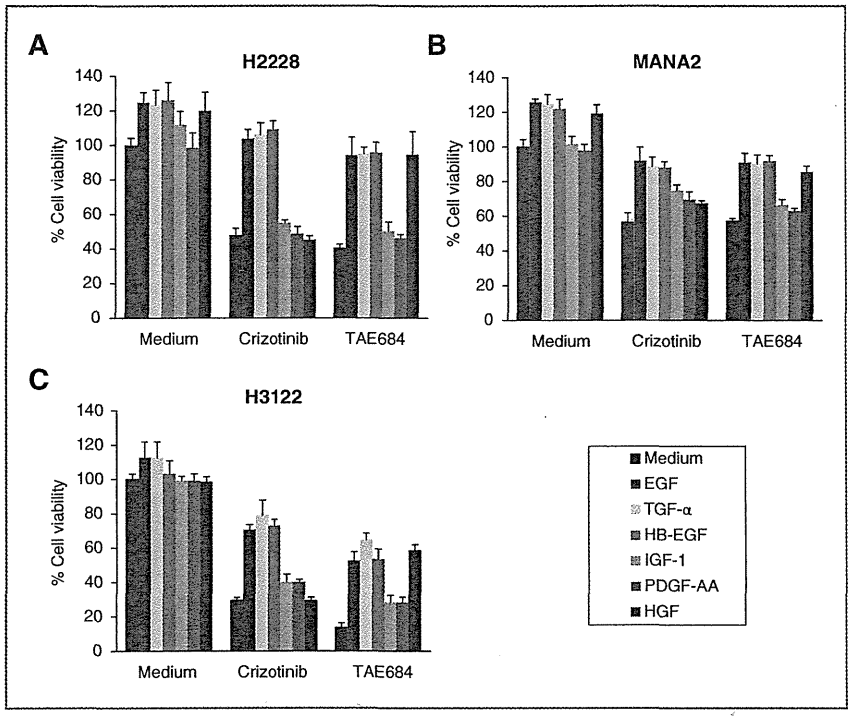

Figure 2. HGF and/or EGFR ligands (EGF, TGF-α, and HB-EGF) reduce the sensitivity of EML4-ALK lung cancer cells to ALK inhibitors *in vitro*. H2228, H3122, and MANA2 cells were incubated with or without crizotinib (100 nmol/L), TAE684 (100 nmol/L), and/or EGF, TGF-α, IGF-I, or PDGF-AA (100 ng/mL); HB-EGF (10 ng/mL), or HGF (50 ng/mL), with cell growth determined after 72 hours. The percentage growth is shown relative to untreated controls. Each sample was assayed in triplicate, with each experiment repeated at least 3 times independently.

assessed the ability of crizotinib to induce apoptosis in H2228 and H3122 cells, we found that crizotinib induced apoptosis in H3122, but not H2228, cells (Supplementary Fig. S3).

HGF and EGFR ligands trigger ALK inhibitor resistance via Met and EGFR, respectively

To assess the mechanism by which these growth factors reduced cell sensitivity to ALK inhibitors, we analyzed the phosphorylation status of ALK, receptors, and their downstream molecules in H2228, H3122, and MANA2 cells by Western blotting. Crizotinib inhibited ALK phosphorylation, thereby suppressing the phosphorylation of Akt, Erk1/2 and STAT-3, as described (ref. 11; Fig. 3A, Supplementary Fig. S4). The EGFR ligands, EGF, TGF-α, and HB-EGF stimulated EGFR phosphorylation. Crizotinib inhibited ALK and STAT-3 phosphorylation even in the presence of EGFR ligands, but failed to inhibit phosphorylation of EGFR and downstream Akt, and Erk1/2. Phosphorylation of ErbB4, a potential receptor for HB-EGF, was not affected by crizotinib or EGFR ligands. To further confirm the involvement of EGFR in crizotinib resistance induced by EGFR ligands, we knocked down EGFR by specific siRNAs in H2228 and H3122 cells (Fig. 3B). Although crizotinib markedly inhibited cell viability and all 3 EGFR ligands induced resistance in cells treated with scrambled siRNA, resistance to crizotinib was not induced by EGF, TGF-α, or HB-EGF in EGFR siRNA-treated cells, indicating that EGFR ligand-triggered crizotinib resistance is mediated by EGFR.

In parallel experiments, TAE684 inhibited ALK phosphorylation, thereby suppressing the phosphorylation of Akt, Erk1/2, and STAT-3 (Fig. 3C). HGF stimulated the phosphorylation of Met and its adaptor protein, Gab1, as described (29). TAE684 inhibited ALK and STAT-3 phosphorylation even in the presence of HGF, but failed to inhibit phosphorylation of Met and downstream Akt and Erk1/2. Phosphorylation of ErbB3, an adaptor of amplified, but not HGF-stimulated Met (30), was not affected by TAE684 or HGF. To further confirm the involvement of Met and Gab1 in HGF-induced TAE684 resistance, we knocked down Met, ErbB3, or Gab1 by specific siRNAs in H2228 and H3122 cells (Fig. 3D). TAE684 markedly inhibited the viability and HGF induced resistance in cells treated with scrambled siRNA. Importantly, treatment of cells with Met or Gab1, but not ErbB3, siRNA, induced TAE684 resistance, indicating the involvement of Met/Gab1 in HGF-induced resistance to TAE684.

Cross-talk of endothelial cells and fibroblasts reduces the sensitivity of EML4-ALK lung cancer cells to ALK inhibitors

To determine which types of host cells could produce EGFR ligands and HGF, we investigated production of these growth factors by various types of host stromal cells, comparing lung epithelial cells and cancer cells. The endothelial cell lines HMVEC produced discernible levels of EGFR ligands, including EGF, TGF-α, and HB-EGF, whereas fibroblasts produced a high level of HGF (Fig. 4A). EML4-ALK lung cancer cells (H2228, H3122, and

Published OnlineFirst May 2, 2012; DOI:10.1158/1078-0432.CCR-11-2972

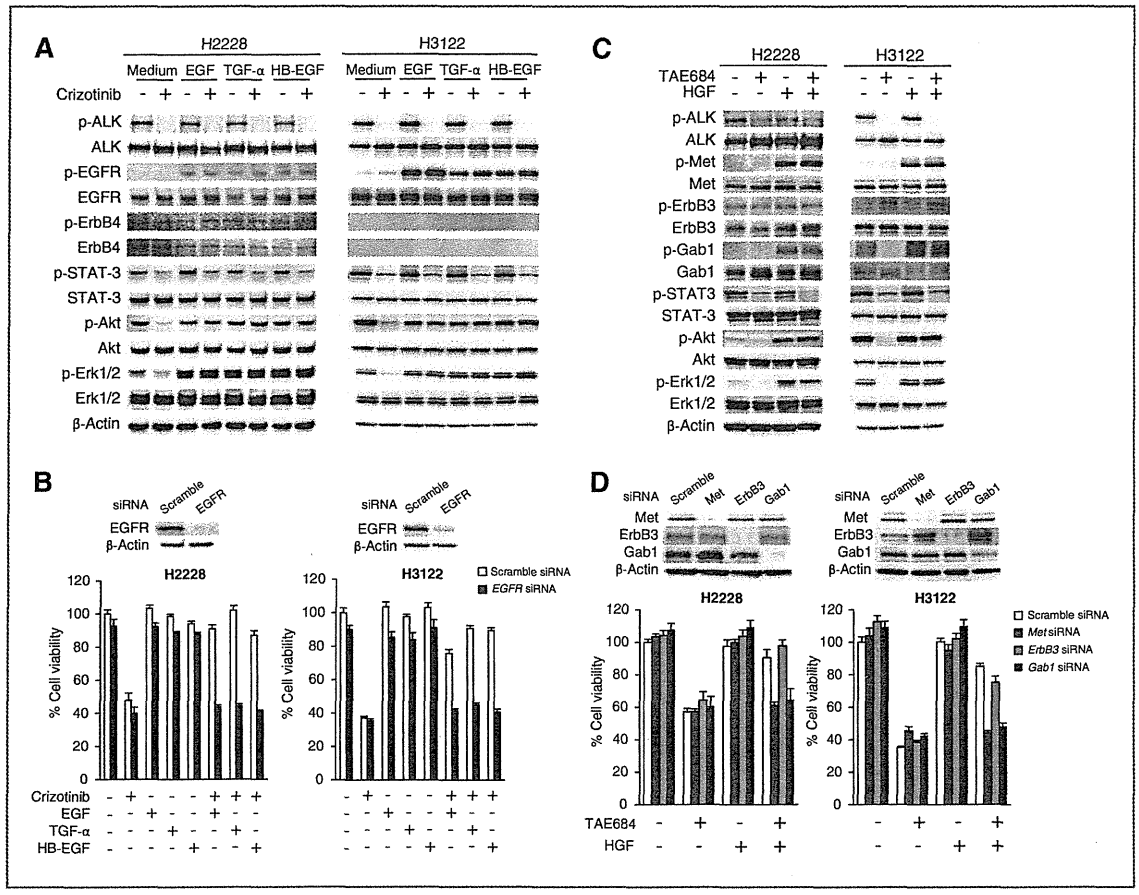

Figure 3. HGF and EGFR ligands trigger ALK inhibitor resistance via Met/Gab1 and EGFR, respectively. A, crizotinib inhibited the phosphorylation of ALK and STAT-3 but not that of EGFR, Akt, and Erk1/2 in the presence of EGF, TGF-α, or HB-EGF. Tumor cells were treated with or without crizotinib (100 nmol/L) for 1 hour and/or EGF (100 ng/mL), TGF-α (100 ng/mL), or HB-EGF (10 ng/mL) for 15 minutes. The cells were lysed and the indicated proteins were detected by immunoblotting. The results shown are representative of 3 independent experiments. B, control or *EGFR*-specific siRNAs were introduced into H2228 and H3122 cells. After 24 hours, the cells were incubated with or without crizotinib (100 nmol/L), and/or EGF (100 ng/mL), TGF-α (100 ng/mL), or HB-EGF (10 ng/mL) for 72 hours and lung cancer cell growth was determined by MTT assays. *EGFR* knockdown was confirmed by immunoblotting. The percentage of growth is shown relative to untreated controls. Each sample was assayed in triplicate, with each experiment repeated at least 3 times independently. C, TAE684 inhibited the phosphorylation of ALK and STAT-3, but not that of Met, Gab1, Akt, and Erk1/2 in the presence of HGF. Tumor cells were treated with or without TAE684 (100 nmol/L) for 1 hour and/or HGF (50 ng/mL) for 15 minutes. The cells were lysed and the indicated proteins were detected by immunoblotting. The results shown are representative of 3 independent experiments. D, control or *Met*, *ErbB3*, or *Gab1*-specific siRNAs were introduced into H2228 and H3122 cells. After 24 hours, the cells were incubated with or without TAE684 (100 nmol/L) and/or HGF (50 ng/mL) for 72 hours and lung cancer cell growth was determined by MTT assays. *Met*, *Gab1*, and *ErbB3* knockdowns were confirmed by immunoblotting. The percentage of growth is shown relative to untreated controls. Each sample was assayed in triplicate, with each experiment repeated at least 3 times independently.

MANA2) and lung epithelial cells (BEAS-2B) produced low or no detectable levels of EGFR ligands or HGF. Interestingly, coculture of H2228 or H3122 cells with fibroblasts (MRC-5) significantly reduced their sensitivity to TAE684, an effect abrogated by anti-HGF antibody (Fig. 4B). Coculture with endothelial cells (HMVEC) also reduced sensitivity to crizotinib, an effect inhibited by anti-EGFR antibody (Fig. 4C).

These results suggested that host stromal cells, such as endothelial cells and fibroblasts, may regulate sensitivity to ALK inhibitors by secreting EGFR ligands and HGF, respectively.

HGF derived from fibroblasts induces TAE684 resistance of EML4-ALK lung cancer cells *in vivo*

To investigate whether sensitivity to TAE684 could be affected by fibroblasts *in vivo*, we subcutaneously inoculated H2228 cells, with or without MRC-5 cells, into SCID mice. The tumors of mice injected with H2228 and MRC-5 cells grew slightly faster than those of mice injected with

Published OnlineFirst May 2, 2012; DOI:10.1158/1078-0432.CCR-11-2972

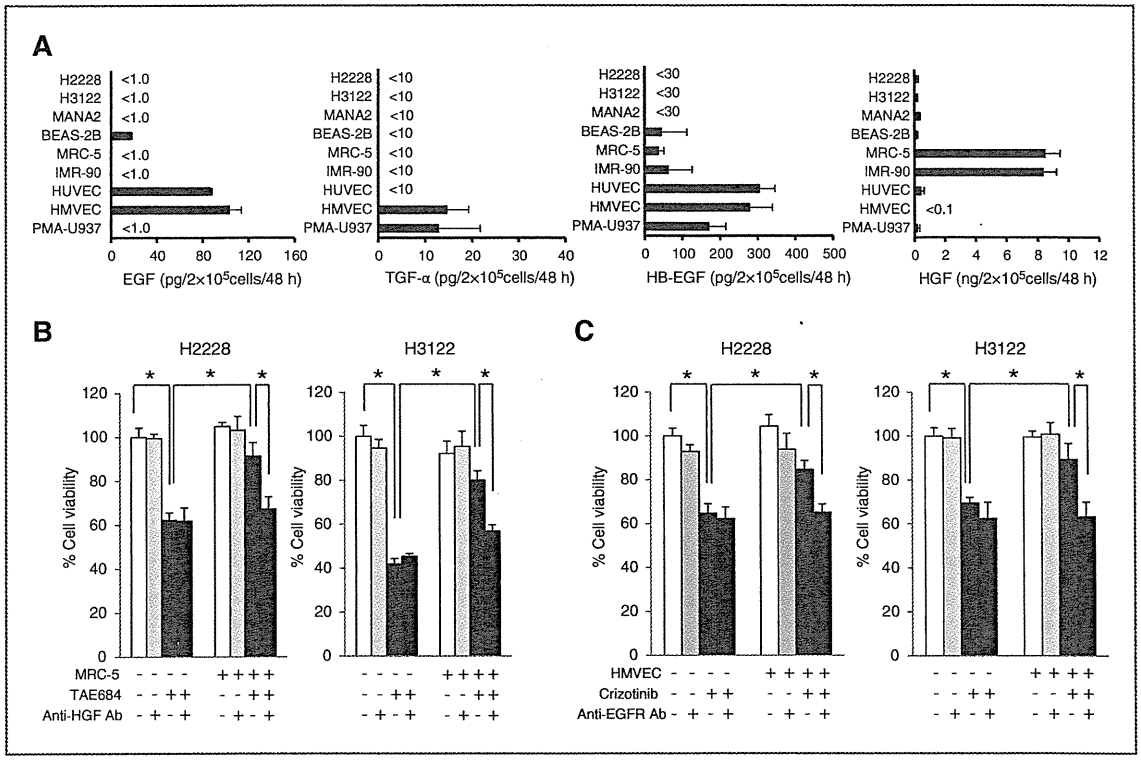

Figure 4. Cross-talk of endothelial cells and fibroblasts reduces sensitivity of EML4-ALK lung cancer cells to ALK inhibitors. A, receptor ligand production was assayed in lung cancer (H2228, H3122, and MANA2), human bronchial epithelial cell (BEAS-2B), fibroblasts (MRC-5 and IMR-90), endothelial cells (HUVEC and HMVEC), and the macrophage differentiated cell line (PMA-U937). The cells were incubated in medium for 48 hours, culture supernatants were harvested, and EGF, TGF-α, HB-EGF, and HGF concentrations were determined by ELISA. All samples were assayed in triplicate. B, H2228 and H3122 cells were cocultured with or without fibroblasts, MRC-5 cells, and/or anti-HGF–neutralizing antibody (2 μg/mL), in the presence or absence of TAE684 (100 nmol/L) for 72 hours, with cell growth determined by MTT assays. *, $P < 0.05$ (one-way ANOVA). Each experiment included triplicate determinations, and each experiment was repeated at least 3 times independently. C, endothelial cell–derived EGFR ligands induced crizotinib resistance in lung cancer cells with EML4-ALK fusion protein, an induction abrogated by blockade of EGFR. H2228 and H3122 cells were cocultured with or without endothelial cells, HMVECs, and/or anti-EGFR–neutralizing antibody (2 μg/mL) in the presence or absence of crizotinib (100 nmol/L) for 72 hours, with cell growth determined as in B. *, $P < 0.05$ (one-way ANOVA). Each experiment included triplicate determinations, with each experiment repeated at least 3 times independently.

H2228 cells alone, but the difference was not statistically significant by day 8 (Fig. 5A). TAE684 treatment, beginning on day 4, caused marked regression of tumors in mice injected with H2228 cells alone, but not of tumors in mice injected with H2228 and MRC-5 cells, indicating that fibroblasts induced resistance to TAE684 *in vivo* (Fig. 5A). We confirmed that HGF was produced by MRC-5 cells *in vivo*. Although the tumors of mice injected with H2228 cells alone did not produce detectable levels of HGF, the tumors of mice injected with H2228 and MRC-5 cells produced high levels of HGF, started on day 4, but decreasing slightly on day 8 (Fig. 5B).

We further analyzed whether coinjection of MRC-5 cells restored the Akt pathway inhibited by TAE684 in the tumors. Western blotting showed that TAE684 treatment inhibited Akt phosphorylation, which was restored by coinjection of MRC-5 cells (Fig. 5C). These results suggested that fibroblasts produced HGF in the tumors and restored Akt phosphorylation as a survival signal, as well as inducing resistance to TAE684 in EML4-ALK lung cancer cells *in vivo*.

Ligand-triggered resistance to ALK inhibitors is abrogated by inhibitors of both HGF-Met and EGFR

To establish novel strategies to treat EGFR ligand- or HGF-triggered resistance to ALK inhibitors, we examined the effect of combinations of ALK inhibitors with EGFR inhibitors (anti-EGFR Abs and reversible EGFR-TKIs) and HGF-Met inhibitors (anti-HGF Abs and Met-TKIs). Combined treatment with erlotinib, a reversible EGFR-TKI and cetuximab, an anti-EGFR Ab, successfully resensitized H2228 and H3122 cells to crizotinib even in the presence of the EGFR ligands, EGF (Fig. 6A), TGF-α (Fig. 6B), and HB-EGF (Fig. 6C). Moreover, the combination of HGF with E7050 (Met-TKI) or anti-HGF Ab resensitized cells to TAE684 (Fig. 6D).

Published OnlineFirst May 2, 2012; DOI:10.1158/1078-0432.CCR-11-2972

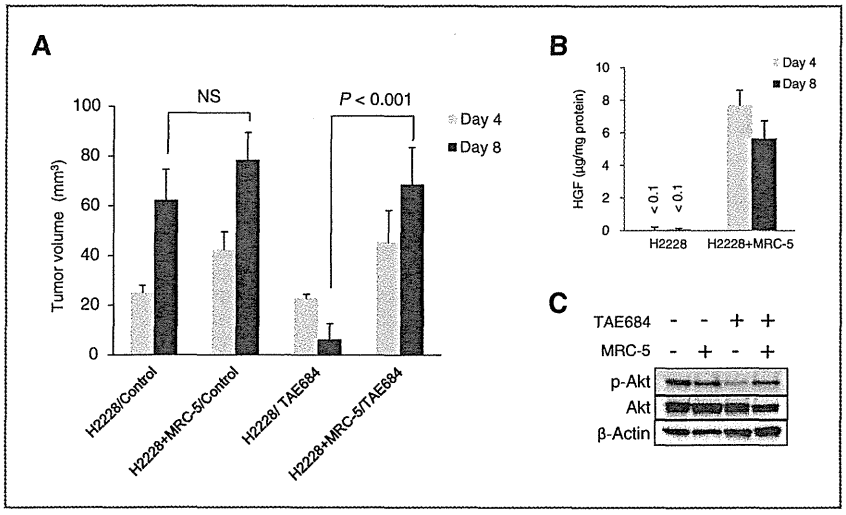

Figure 5. HGF derived from fibroblasts induces TAE684 resistance of EML4-ALK lung cancer cells *in vivo*. A, fibroblast-derived HGF induced TAE684 resistance in H2228 tumors in SCID mice. H2228 cells (5×10^6), with or without MRC-5 cells (5×10^6), were inoculated subcutaneously into SCID mice on day 0. Starting on day 4, mice received oral TAE684 (1.25 mg/kg/d) or vehicle alone, with tumor size measured on days 4 and 8. Tumor volumes were calculated as described in Materials and Methods. Data shown are the representative of 2 independent experiments. Error bars indicate SEs of 6 mice. $P < 0.05$ was considered significant by one-way ANOVA. NS, not significant. B, HGF production by tumor tissues. Tumors were harvested on days 4 and 8 and lysed, and HGFs in the lysates were assayed by ELISA. All samples were assayed in triplicate. C, fibroblast-derived HGF induced TAE684 resistance via the Akt signal pathway *in vivo*. Tumors were harvested 2 hours after treatment on day 7 and lysed, and the lysates were analyzed by immunoblotting with the indicated antibodies, as described in Materials and Methods. The results shown are representative of 2 independent experiments.

Discussion

We have shown here that endothelial cells and fibroblasts, both components of the tumor microenvironment, secreted EGFR ligands and HGF, respectively, causing resistance to the ALK inhibitors crizotinib and/or TAE684 by activating bypass survival signals.

Of the EGFR ligands, EGF and TGF-α bind predominantly to EGFR, whereas HB-EGF binds to EGFR and ErbB4 (17). H2228 cells expressed both EGFR and ErbB4. Our results suggested that the bypass survival signal induced by EGFR ligands is mediated mainly by EGFR, as EGFR ligands markedly activated the phosphorylation of EGFR, not ErbB4. Moreover, knockdown of EGFR abrogated resistance caused by all EGFR ligands tested. EGFR ligand–triggered resistance was canceled by erlotinib or cetuximab, an anti-EGFR Ab, drugs approved for the treatment of patients with NSCLC and colorectal cancer. In addition, AP26113, an inhibitor of both ALK and EGFR, has been reported active against *EML4-ALK* lung cancer cells with amplified *ALK* and secondary mutations (7). Therefore, clinical trials are warranted to evaluate the efficacy and feasibility of combinations of an ALK inhibitor and these EGFR inhibitors to overcome ALK inhibitor resistance.

HGF, the sole ligand of Met (29), is important in EGFR-TKI resistance in *EGFR*-mutant lung cancer. HGF derived from cancer cells or stromal fibroblasts activated Met phosphorylation and stimulated the downstream Akt and Erk1/2 pathways (21, 22, 30) using Gab1, an adaptor protein for Met (31), triggering resistance to both reversible and irreversible EGFR-TKIs. In our Japanese cohort study of patients with *EGFR*-mutant lung cancer, high HGF expression was detected in 61% of tumors with acquired resistance and in 29% of tumors with intrinsic resistance to EGFR-TKIs, suggesting the rationale of targeting HGF to overcome EGFR-TKI resistance (32). We also found that HGF triggered TAE684 resistance by activating Met and stimulating downstream Akt and Erk1/2 pathways using the adaptor protein Gab1. Because many anti-HGF Abs and Met-TKIs are being evaluated in clinical trials, HGF-triggered resistance to selective ALK inhibitors may be controlled by their combinations in the near future.

EGFR and Met have been shown to interact with each other and to mediate redundant signaling in lung cancer cells (33). In *EGFR*-mutant lung cancer cells, *Met* amplification causes EGFR-TKI resistance by triggering bypass survival signals using ErbB3, an adaptor protein (34). Met activation by HGF also triggers resistance to EGFR-TKIs that use Gab1 as an adaptor. In *EML4-ALK* lung cancer cells, both novel ALK second mutations and autocrine EGFR activation causes resistance to ALK inhibitors (11). We found that paracrine HGF and EGFR ligands could trigger ALK inhibitor resistance. Taken together, these findings suggest that signaling by EGFR and Met is crucial for the survival of lung cancer cells with *EGFR* mutations and *EML4-ALK* translocations under inhibition of these driver oncogenes.

We found that resistance to TAE684 was induced by both EGFR ligands and HGF, whereas crizotinib resistance was induced by EGFR ligands alone, a finding that may be due to the dual activities of crizotinib on ALK and

Published OnlineFirst May 2, 2012; DOI:10.1158/1078-0432.CCR-11-2972

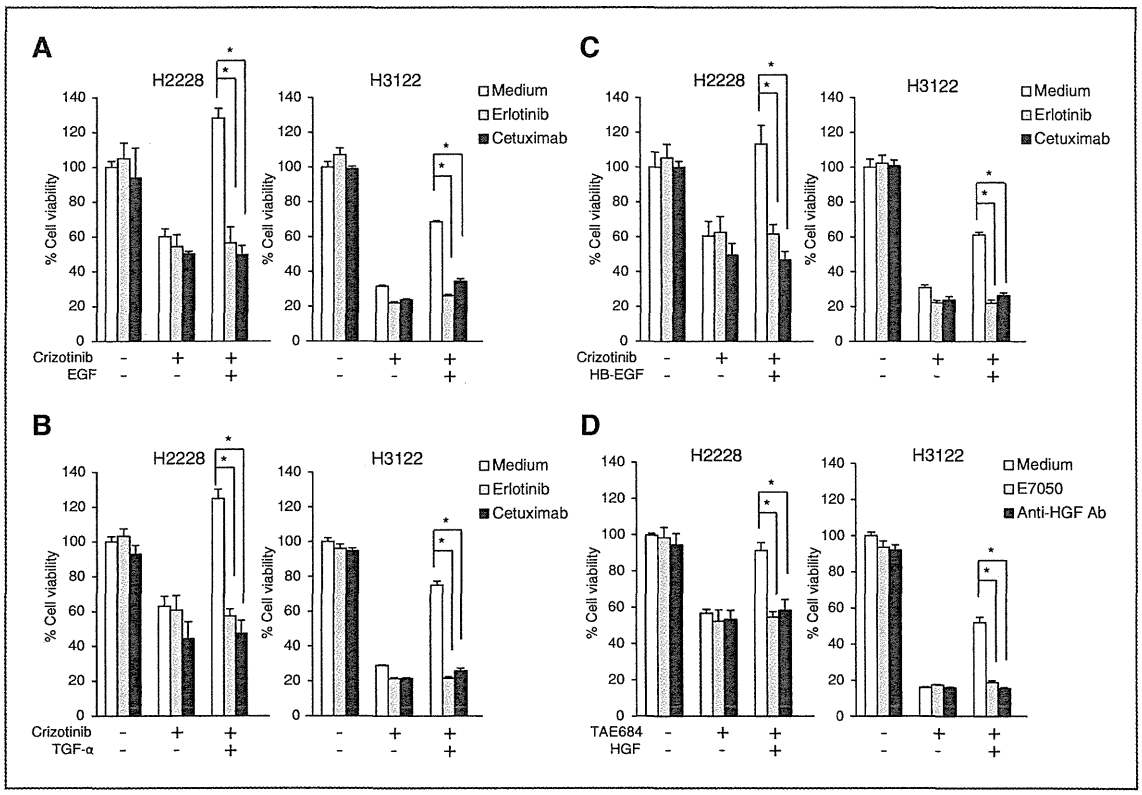

Figure 6. Ligand-triggered resistance to ALK inhibitors is abrogated by inhibitors of both HGF-Met and EGFR. A–C, the EGFR inhibitors erlotinib and cetuximab abrogated EGFR ligand-induced crizotinib resistance in EML4-ALK lung cancer cells. H2228 and H3122 cells were treated for 72 hours with or without crizotinib (100 nmol/L) and/or EGF (100 ng/mL), TGF-α (100 ng/mL), or HB-EGF (10 ng/mL) in the presence or absence of erlotinib (1 μmol/L) or cetuximab (2 μg/mL). Cell growth was determined by MTT assays. *, $P < 0.01$ (one-way ANOVA). Each experiment included triplicate determinations, and each experiment was repeated at least 3 times independently. D, Met-TKI E7050 or Anti-HGF antibody abrogated HGF-induced TAE684 resistance in EML4-ALK lung cancer cells. H2228 and H3122 cells were treated for 72 hours with or without TAE684 (100 nmol/L) and/or HGF (50 ng/mL) in the presence or absence of E7050 (1 μmol/L) or anti-HGF–neutralizing antibody (2 μg/mL). Cell growth was determined by MTT assays. *, $P < 0.01$ (one-way ANOVA). Each experiment included triplicate determinations, and each experiment was repeated at least 3 times independently.

Met (5). Selective ALK inhibitors are expected to be effective against *EML4-ALK* lung cancer cells, even after acquiring *ALK* amplification and *ALK* second mutations and becoming refractory to crizotinib (7, 35). Our findings, however, suggest that HGF-triggered resistance may be directed against selective ALK inhibitors, not crizotinib. Future clinical trials with selective ALK inhibitors may reveal the class of ALK inhibitors that is more beneficial for *EMK4-ALK* lung cancer patients.

EML4-ALK- and *EGFR*-mutant lung cancers show dramatic responses to ALK inhibitors and EGFR-TKIs, respectively (5, 36, 37). Complete responses, however, are rarely achieved, despite these cells express the target (EML4-ALK or mutant EGFR) of the drug. Low expression of BIM, a proapoptotic molecule, may explain, at least in part, the variations in sensitivity of *EGFR*-mutant lung cancer to EGFR-TKIs (38). This heterogeneous sensitivity may also be explained by HGF, as HGF is expressed more or less equally in *EGFR*-mutant lung tumors sensitive to EGFR-TKIs (32). Therefore, EGFR ligands in EML4-ALK lung tumors may be involved in their heterogeneous response to crizotinib. It is also curious whether ligand-triggered resistance is an independent mechanism or one that provided partial resistance when combined with another mechanism. Because crizotinib is expected to be approved in Japan to treat EML4-ALK lung cancer in 2012, we are planning a study to assess this possibility in clinical specimens.

In conclusion, we found that receptor ligands, such as EGFR ligands and HGF, could cause resistance to the ALK inhibitors crizotinib and/or TAE684 by activating bypass survival signals. These ligands and growth factors may be produced by host stromal cells, which constitute the cancer microenvironment. Paracrine HGF from stromal fibroblasts may also trigger resistance to EGFR-TKIs in EGFR-mutant lung cancer cells by activating bypass signals (22). Collectively, these observations suggest that paracrine receptor activation by the microenvironment

Published OnlineFirst May 2, 2012; DOI:10.1158/1078-0432.CCR-11-2972

may be an important mechanism inducing resistance to molecular targeted drugs in oncogene-activated lung cancer cells. These findings suggest that targeting of receptor ligands may result in more successful therapy in lung cancer.

Disclosure of Potential Conflicts of Interest

S. Yano received honoraria from Chugai Pharma and AstraZeneca and research fundings from Chugai Pharma and Eisai co., ltd. H. Mano received honoraria from Pfizer Inc., and T. Nakagawa and T. Uenaka are employees of Eisai co., ltd. The other authors disclosed no potential conflicts of interest.

Authors' Contributions

Conception and design: T. Yamada, S. Takeuchi, S. Yano
Development of methodology: T. Yamada
Analysis and interpretation of data (e.g., statistical analysis, biostatistics, computational analysis): T. Yamada, H. Mano
Acquisition of data (provided animals, acquired and managed patients, provided facilities, etc.): K. Kita, T. Nakagawa, T. Uenaka
Writing, review, and/or revision of the manuscript: T. Yamada, S. Yano
Administrative, technical, or material support (i.e., reporting or organizing data, constructing databases): J. Nakade, S. Nanjo, T. Nakamura, K. Matsumoto, M. Soda, H. Mano, S. Yano
Study supervision: S. Yano

Acknowledgments

The authors thank Dr. Jeffrey A. Engelman (Massachusetts General Hospital Cancer Center) for providing the H3122 cells.

Grant Support

This study was supported by grants-in-aid for cancer research (T. Yamada, 23790902 and S. Yano, 21390256) and scientific research on innovative areas "Integrative Research on Cancer Microenvironment Network" (S. Yano, 22112010A01) from the Ministry of Education, Culture, Sports, Science, and Technology of Japan.

The costs of publication of this article were defrayed in part by the payment of page charges. This article must therefore be hereby marked *advertisement* in accordance with 18 U.S.C. Section 1734 solely to indicate this fact.

Received November 21, 2011; revised March 28, 2012; accepted April 17, 2012; published OnlineFirst May 2, 2012.

References

1. Soda M, Choi YL, Enomoto M, Takada S, Yamashita Y, Ishikawa S, et al. Identification of the transforming EML4-ALK fusion gene in non-small-cell lung cancer. Nature 2007;448:561–6.
2. Horn L, Pao W. EML4-ALK: honing in on a new target in non-small-cell lung cancer. J Clin Oncol 2009;27:4232–5.
3. Koivunen JP, Mermel C, Zejnullahu K, Murphy C, Lifshits E, Holmes AJ, et al. EML4-ALK fusion gene and efficacy of an ALK kinase inhibitor in lung cancer. Clin Cancer Res 2008;14:4275–83.
4. Choi YL, Takeuchi K, Soda M, Inamura K, Togashi Y, Hatano S, et al. Identification of novel isoforms of the EML4-ALK transforming gene in non-small cell lung cancer. Cancer Res 2008;68:4971–6.
5. Kwak EL, Bang YJ, Camidge DR, Shaw AT, Solomon B, Maki RG, et al. Anaplastic lymphoma kinase inhibition in non-small-cell lung cancer. N Engl J Med 2010;363:1693–703.
6. Choi YL, Soda M, Yamashita Y, Ueno T, Takashima J, Nakajima T, et al. ALK Lung Cancer Study Group. EML4-ALK mutations in lung cancer that confer resistance to ALK inhibitors. N Engl J Med 2010;363:1734–9.
7. Katayama R, Khan TM, Benes C, Lifshits E, Ebi H, Rivera VM, et al. Therapeutic strategies to overcome crizotinib resistance in non-small cell lung cancers harboring the fusion oncogene EML4-ALK. Proc Natl Acad Sci U S A 2011;108:7535–40.
8. Sasaki T, Okuda K, Zheng W, Butrynski J, Capelletti M, Wang L, et al. The neuroblastoma-associated F1174L ALK mutation causes resistance to an ALK kinase inhibitor in ALK-translocated cancers. Cancer Res 2010;70:10038–43.
9. Doebele RC, Pilling AB, Aisner DL, Kutateladze TG, Le AT, Weickhardt AJ, et al. Mechanisms of resistance to crizotinib in patients with ALK gene rearranged non-small cell lung cancer. Clin Cancer Res 2012;18:1472–82.
10. Katayama R, Shaw AT, Khan TM, Mino-Kenudson M, Solomon BJ, Halmos B, et al. Mechanisms of acquired crizotinib resistance in ALK-rearranged lung Cancers. Sci Transl Med 2012;4:120ra17.
11. Sasaki T, Koivunen J, Ogino A, Yanagita M, Nikiforow S, Zheng W, et al. A novel ALK secondary mutation and EGFR signaling cause resistance to ALK kinase inhibitors. Cancer Res 2011;71:6051–60.
12. Heuckmann JM, Hölzel M, Sos ML, Heynck S, Balke-Want H, Koker M, et al. ALK mutations conferring differential resistance to structurally diverse ALK inhibitors. Clin Cancer Res 2011;17:7394–401.
13. McAllister SS, Weinberg RA. Tumor-host interactions: a far-reaching relationship. J Clin Oncol 2010;28:4022–8.
14. Joyce JA, Pollard JW. Microenvironmental regulation of metastasis. Nat Rev Cancer 2009;9:239–52.
15. Seruga B, Zhang H, Bernstein LJ, Tannock IF. Cytokines and their relationship to the symptoms and outcome of cancer. Nat Rev Cancer 2008;8:887–99.
16. Janku F, Stewart DJ, Kurzrock R. Targeted therapy in non-small-cell lung cancer–is it becoming a reality? Nat Rev Clin Oncol 2010;7:401–14.
17. Yasumoto K, Yamada T, Kawashima A, Wang W, Li Q, Donev IS, et al. The EGFR ligands amphiregulin and heparin-binding egf-like growth factor promote peritoneal carcinomatosis in CXCR4-expressing gastric cancer. Clin Cancer Res 2011;17:3619–30.
18. Matsumoto K, Nakamura T. Hepatocyte growth factor and the Met system as a mediator of tumor-stromal interactions. Int J Cancer 2006;119:477–83.
19. Masuya D, Huang C, Liu D, Nakashima T, Kameyama K, Haba R, et al. The tumour-stromal interaction between intratumoral c-Met and stromal hepatocyte growth factor associated with tumour growth and prognosis in non-small-cell lung cancer patients. Br J Cancer 2004;90:1555–62.
20. Meert AP, Martin B, Delmotte P, Berghmans T, Lafitte JJ, Mascaux C, et al. The role of EGF-R expression on patient survival in lung cancer: a systematic review with meta-analysis. Eur Respir J 2002;20:975–81.
21. Yamada T, Matsumoto K, Wang W, Li Q, Nishioka Y, Sekido Y, et al. Hepatocyte growth factor reduces susceptibility to an irreversible epidermal growth factor receptor inhibitor in EGFR-T790M mutant lung cancer. Clin Cancer Res 2010;16:174–83.
22. Wang W, Li Q, Yamada T, Matsumoto K, Matsumoto I, Oda M, et al. Crosstalk to stromal fibroblasts induces resistance of lung cancer to epidermal growth factor receptor tyrosine kinase inhibitors. Clin Cancer Res 2009;15:6630–8.
23. Soda M, Takada S, Takeuchi K, Choi YL, Enomoto M, Ueno T, et al. A mouse model for EML4-ALK-positive lung cancer. Proc Natl Acad Sci U S A 2008;105:19893–7.
24. Nakamura Y, Azuma M, Okano Y, Sano T, Takahashi T, Ohmoto Y, et al. Upregulatory effects of interleukin-4 and interleukin-13 but not interleukin-10 on granulocyte/macrophage colony-stimulating factor production by human bronchial epithelial cells. Am J Respir Cell Mol Biol 1996;15:680–7.
25. Koren HS, Anderson SJ, Larrick JW. *In vitro* activation of a human macrophage-like cell line. Nature 1979;279:328–31.
26. Kuniyasu H, Yano S, Sasaki T, Sasahira T, Sone S, Ohmori H. Colon cancer cell-derived high mobility group 1/amphoterin induces growth inhibition and apoptosis in macrophages. Am J Pathol 2005;166:751–60.
27. Nakagawa T, Tohyama O, Yamaguchi A, Matsushima T, Takahashi K, Funasaka S, et al. E7050: a dual c-Met and VEGFR-2 tyrosine kinase

Cancer Science
The official journal of the Japanese Cancer Association JCA

High-throughput resequencing of target-captured cDNA in cancer cells

Toshihide Ueno,[1,5] Yoshihiro Yamashita,[1,5] Manabu Soda,[1] Kazutaka Fukumura,[2] Mizuo Ando,[2] Azusa Yamato,[1] Masahito Kawazu,[2] Young Lim Choi[1,2] and Hiroyuki Mano[1,2,3,4]

[1]Division of Functional Genomics, Jichi Medical University, Tochigi; [2]Department of Medical Genomics, Graduate School of Medicine, University of Tokyo, Tokyo; [3]CREST Japan Science and Technology Agency, Saitama, Japan

(Received May 30, 2011/Revised September 7, 2011/Accepted September 14, 2011/Accepted manuscript online September 20, 2011/Article first published online October 13, 2011)

The recent advent of whole exon (exome)-capture technology, coupled with second-generation sequencers, has made it possible to readily detect genomic alterations that affect encoded proteins in cancer cells. Such target resequencing of the cancer genome, however, fails to detect most clinically-relevant gene fusions, given that such oncogenic fusion genes are often generated through intron-to-intron ligation. To develop a resequencing platform that simultaneously captures point mutations, insertions–deletions (indels), and gene fusions in the cancer genome, we chose cDNA as the input for target capture and extensive resequencing, and we describe the versatility of such a cDNA-capture system. As a test case, we constructed a custom target-capture system for 913 cancer-related genes, and we purified cDNA fragments for the target gene set from five cell lines of CML. Our target gene set included Abelson murine leukemia viral oncogene homolog 1 (*ABL1*), but it did not include breakpoint cluster region (*BCR*); however, the sequence output faithfully detected reads spanning the fusion points of these two genes in all cell lines, confirming the ability of cDNA capture to detect gene fusions. Furthermore, computational analysis of the sequence dataset successfully identified non-synonymous mutations and indels, including those of tumor protein p53 (*TP53*). Our data might thus support the feasibility of a cDNA-capture system coupled with massively parallel sequencing as a simple platform for the detection of a variety of anomalies in protein-coding genes among hundreds of cancer specimens. (*Cancer Sci* 2012; 103: 131–135)

Cancer is thought to result from various alterations of the genome, including point mutations, insertions–deletions (indels), and genomic rearrangements.[1] Whereas comprehensive sequencing of the cancer genome, or "cancer genome resequencing", is a promising approach to the identification of such anomalies, and to provide a basis for the development of effective treatment strategies for cancer, determination of the nucleotide sequence of the entire human genome with conventional Sanger sequencers remains a highly demanding task. However, the recent advent of massively parallel sequencing systems, or second-generation sequencers, has rendered such projects manageable in private laboratories[2] and triggered the formation of large-scale consortia, such as The Cancer Genome Atlas and International Cancer Genome Consortium,[3] to undertake cancer genome resequencing for hundreds of specimens. Cancer genome resequencing with massively parallel sequencers has already provided a wealth of information on genome-wide mutation status for melanoma,[4] acute myeloid leukemia,[5] hepatocellular carcinoma,[6] and other cancers.

Even with the current massively parallel sequencers, however, the determination and compilation of the full genome sequence for a given sample might still take almost 1 month. Comparison of the cancer genome among many specimens thus remains time-consuming and labor intensive. Anomalies in protein-coding genes likely play a major role in carcinogenesis. Given that exonic regions occupy only ~1.3% of the human genome, sequencing such targeted regions would be expected to markedly facilitate the discovery of proteins that are activated or inactivated specifically in cancer cells. Indeed, target-capture strategies, coupled with massively parallel sequencers, have revealed important genetic changes in cancer,[7] as well as in hereditary disorders.[8,9]

One important drawback of such target-capture approaches, however, is their inability to detect gene fusions. Most cancer-associated gene fusion events occur within introns (resulting in exon-to-exon ligation in the corresponding mRNA), and exon capture does not reveal breakage and ligation of intronic regions. Recurrent gene fusions were once thought to be rare in epithelial tumors compared with hematologic malignancies and sarcomas;[10] however, our recent discovery of the echinoderm microtubule associated protein like-4 (EML4)-anaplastic lymphoma kinase (ALK) fusion gene in lung cancer and the discovery by others of rearrangements in loci for the v-ets avian erythroblastosis virus E26 oncogene homolog (ETS) family of transcription factors in prostate cancer have led to a revision of this notion.[11,12] It would thus be desirable to develop a resequencing platform that is able to capture, within a reasonable timeframe, all gene fusions, point mutations, and indels in the cancer genome. In pursuit of this goal, we have now examined the efficacy of high-throughput sequencing of captured cDNA for the identification of such cancer genome anomalies.

Materials and Methods

Cell lines. Cell lines established from the blast crisis stage of CML, including MEG-01s, KCL-22-SR, K562, NCO2, and KU812,[13,14] were obtained from the Japanese Collection of Research Bioresources (Osaka, Japan) and were maintained in RPMI-1640 medium (Invitrogen, Carlsbad, CA, USA) supplemented with 10% FBS (Invitrogen). Total RNA was isolated from each cell line with the use of an RNeasy mini kit (Qiagen, Valencia, CA, USA) and was subjected to cDNA synthesis with an oligo(dT) primer.

Gene expression profiling. The cDNA prepared from total poly(A)-RNA of KCL-22-SR cells was subjected to hybridization with the HGU95Av2 microarray (Affymetrix, Santa Clara, CA, USA), as described previously.[15] The expression intensity of each test gene on the array was normalized by the 50th percentile value.

cDNA-capture methods. RNA probes of 120 bases were designed to cover (with a 60-base overlap) cDNA of 913 human protein-coding genes (Table S1), and were synthesized by Agilent Technologies (Santa Clara, CA, USA). During the design of the probes, the Repeat Masker dataset (http://www.repeatmasker.org) was used to remove probes corresponding to

[4]To whom correspondence should be addressed. E-mail: hmano@jichi.ac.jp
[5]These authors contributed equally to this work.

doi: 10.1111/j.1349-7006.2011.02105.x

repetitive sequences in the human genome. Hybridization of DNA fragments to the RNA probes was performed according to the protocols recommended for the SureSelect Target Enrichment system (Agilent). We also used the SureSelect Human X Chromosome Demo kit (Agilent) to examine purification efficiency. Purified DNA fragments were then subjected to sequencing with a Genome Analyzer IIx (GAIIx; Illumina, San Diego, CA, USA) for 76 bases from both ends by the paired-end sequencing system.

Computational pipeline. Raw read data were quality filtered on the basis of the presence of the Illumina adaptor sequences and a *Q*-value of ≥20. The resulting read sequences were then subjected to an in-house computational pipeline to identify various mutations (Fig. S1). In brief, read sequences were matched with the Bowtie algorithm[16] to the cDNA sequences of the 913 genes used to construct our custom-made SureSelect system. The matched reads were then examined for the presence of non-synonymous mutations and single nucleotide polymorphisms (SNP) deposited in dbSNP (build 132, http://www.ncbi.nlm.nih.gov/projects/SNP/index.html). The remaining reads were further matched to the cDNA sequences with Burrows-Wheeler Aligner (BWA) and Basic Local Alignment Search Tool (BLAST) algorithms to search for indels and multiple mutations.[17,18] Candidates for non-synonymous mutations were identified only when ≥20% of reads correspond to the mutations at positions with ≥50 coverage.

For the selection of reads corresponding to possible fusion cDNA, nucleotide sequences of 20 bp were obtained from both ends of each read and were separately matched to RefSeq mRNA (http://www.ncbi.nlm.nih.gov), KnownGeneMrna,[19] and the human genome sequence (GRCh37, http://www.ncbi.nlm.nih.gov/projects/genome/assembly/grc/human/data/?build=37). Reads were considered to be derived from fusion genes if the ends of a given read matched to different genes within the 913-gene group, or one end matched to a single gene within the 913-gene group and the other end matched to a sequence in RefSeq, KnownGeneMrna, or the human genome sequence that did not correspond to the 913 genes. Candidates for fusion genes were identified only when four or more reads were mapped to possible fusion points.

RT–PCR. To confirm the presence of an alternatively-spliced mixed-lineage leukemia (*MLL*) mRNA, we subjected oligo(dT)-primed cDNA of KU812 cells to PCR with the combination of the F-1 primer (5′-ACCTCGTGGGAGACCTAGAAGTGG-3′) and the R primer (5′-AGTCATTGGAAGCTTGTCTGCCTG-3′), or with the combination of the F-2 primer (5′-CCTGTGGGTAGGGTTTCCAAAGAG-3′) and the R primer.

Results

Efficiency of cDNA-capture sequencing. Paired-end sequencing of target-captured cDNA was briefly described in a previous study;[20] however, how the efficiency of target purification with cDNA compares with that with genomic DNA remains unclear. We therefore attempted to optimize the conditions for cDNA purification with the SureSelect system. Oligo(dT)-primed cDNA of KCL-22-SR cells were fragmented to a mean size of 500 or 200 bp and then subjected to purification with the use of the SureSelect Human X Chromosome Demo kit, which is designed to capture genomic sequences derived from the human X chromosome. Genomic DNA of KCL-22-SR cells was similarly processed and hybridized with the X Chromosome Demo kit. The purified fragments at either 4 or 8 pM were then sequenced by the GAIIx system.

The X chromosome-mapped cDNA reads occupied 62.1%, 81.6%, 62.4%, and 82.2% of quality filter-passed reads for the experiments with 4 pM of 500-bp fragments, 4 pM of 200-bp fragments, 8 pM of 500-bp fragments, and 8 pM of 200-bp fragments, respectively (Fig. 1). Thus, these results suggested that the shorter cDNA fragments were captured more efficiently than the longer ones. Furthermore, the purification efficiency for genomic DNA fragments was not higher than that for cDNA, irrespective of DNA concentration and fragmentation size (Fig. 1), supporting the feasibility of cDNA-capture approaches.

The ability to detect breakpoint cluster region (*BCR*)-Abelson murine leukemia viral oncogene homolog 1 (*ABL1*) fusion reads was reduced for the cDNA sheared to ~200 bp compared with that for those of ~500 bp (see below). The former cDNA detected 83.7% or 76% of the fusion reads detected by the latter cDNA at input concentrations of 4 and 8 pM, respectively. This result is in line with our computational bootstrap trial (n = 10 000) showing that the number of randomly-fragmented, 200-bp reads encompassing the *BCR–ABL1* fusion point is ~2.5 times higher than that of 500-bp reads (data not shown). However, given that the total number of high-quality reads was much higher in the data for the 200-bp cDNA than in those for the 500-bp cDNA (Fig. 1), we chose to use 8 pM of cDNA with a mean size of 200 bp for further experiments.

Custom cDNA-capture system. We also tested whether extensive sequencing of cDNA generated from total poly(A)-RNA (unselected cDNA) might serve to identify gene fusions, point mutations, and indels. For this purpose, unselected cDNA were prepared from KCL22-SR cells, and subjected to GAIIx sequencing, yielding 34.1 million reads, which mapped to 36 128 RefSeq entries (data not shown). The distribution of read number per transcript in the data is shown in Figure 2a. Among the 36 128 entries, only 200 (0.55%) accounted for ~20% of total reads, and 4.55% accounted for ~50% of reads. Thus, as expected, resequencing data for unselected cDNA consist mostly of reads corresponding to a limited number of highly-abundant transcripts.

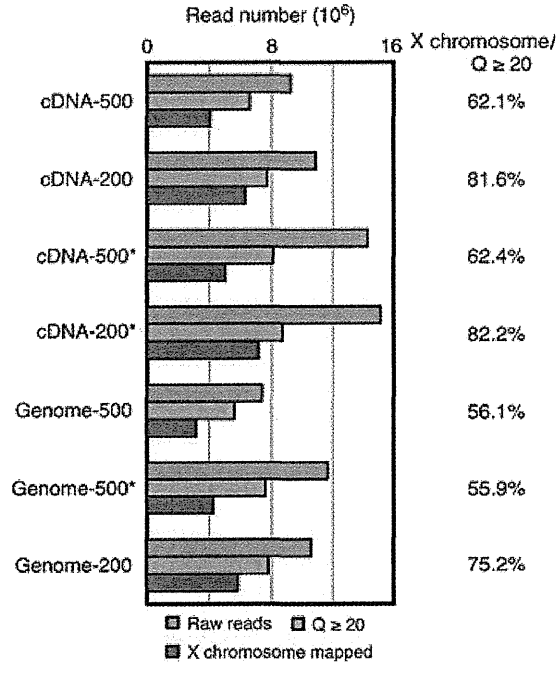

Fig. 1. Comparison of capture efficiency between cDNA and genomic DNA. Genomic DNA or cDNA of KCL-22-SR cells was fragmented to a mean size of 200 or 500 bp, and then subjected to purification with the SureSelect Human X Chromosome Demo kit, followed by GAIIx sequencing at a concentration of 4 or 8 pM (the latter indicated by an asterisk). Numbers of raw reads, reads with a *Q*-value of ≥20 ($Q \geq 20$), and reads mapped to the human X chromosome are shown for each experiment. Percentage of X chromosome-mapped reads among the reads with a *Q*-value of ≥20 is shown on the right.

doi: 10.1111/j.1349-7006.2011.02105.x